ABSTRACT

SHAH, ABHILASHA PARAG. Impact of Analyte-Surface Spacing on the Performance of Desorption/Ionization on Porous Silicon Mass Spectrometry (DIOS-MS). (Under the direction of Dr. Lin He.)

Desorption/ionization on porous silicon (DIOS), a matrix-free laser desorption mass spectrometric technique shows potential for direct analysis of biological compounds in the low mass region. However, the geometric scale of the porous silicon is significantly smaller than the biological samples used in MS imaging and suspect to limit an effective direct analysis of analyte. Herein, I have investigated the effect of the spacing distance between analytes and a porous substrate in DIOS-MS. In particular, organic polymer films were used to simulate the biological tissue between analyte and porous substrate. These films circumvent biological complexity that simplifies data analysis. The thicknesses of polymer film on the substrate controlled by varying spin coating condition. Different classes of analytes were used as standard molecules to evaluate the analyte-substrate spacing effect. In all cases, the standard molecules were successfully detected atop of the polymer film in DIOS-MS. The insulating layer of polymer shift the laser threshold compare to bare DIOS. Relatively stable signal-to-background (S/B) ratios across the tested spacing distances suggest that the analyte detection is less dependent of the distance between analyte and porous surface. The total ion current (TIC) of the analytes however, decreases as the distance increases suggesting distance effect on desorption/ionization. Moreover, the TIC was limited by the amount of analyte accessible for detection. In addition, the ultra-thin SiOx film showed improvement in analyte detectability over the tested thickness. Analyte detection on the DIOS surface greatly influence by surface chemical functionality; oxidized surface is advantageous for positive mode detection whereas the amine derivatized surface showed improvement in negative mode detection.

Impact of Analyte-Surface Spacing on the Performance of Desorption/Ionization on Porous Silicon Mass Spectrometry (DIOS-MS)

by
Abhilasha Parag Shah

A thesis submitted to the Graduate Faculty of
North Carolina State University
In partial fulfillment of the
Requirements for the degree of
Master of Science

Chemistry

Raleigh, North Carolina

2008

APPROVED BY:

_____
Assistant Professor Lin He
Chair of Advisory Committee
Chemistry

_____
Professor Morteza Khaledi
Chemistry

_____
Professor Edmond Bowden
Chemistry

DEDICATION

I would like to dedicate this work to my loving husband. Without his constant motivation, understanding, help, patience and most importantly financial support throughout my research, this work would not have been possible. I would also like to dedicate it to my parents, my brother Mrugesh, my sisters Monika & Vaishali and my sister-in-laws & brother-in-laws for their supports in pursuit of my education. Last but not the least to little cuties of my family (Priyal, Aagam, Nandika, Hena & Kavisha) who bring lots of happiness and joys to our lives.

BIOGRAPHY

The author was born in Ahmedabad, India in 1978. After finishing High School, she received a Bachelor Degree in Chemistry from M.G. Science Institute, Gujarat State University (India). The author then went on to be married to Dr. Parag Shah in 2002 and moved USA to accompany her husband. After taking courses at NCSU in Post-Baccalaureate studies, she officially joined the Chemistry Department of NCSU in 2005 in pursuit of a Master of Science degree.

ACKNOWLEDGMENTS

I would like to first and foremost thank my advisor, Dr. Lin He for her patience, excellent guidance, and careful supervision throughout the course of my research and thesis write-up. She has been an essence of inspiration and a model of self-discipline. I would like to acknowledge Dr. Harold Ade at North Carolina State University at physics department for providing access to the spin coater and the ellipsometer. I would like to thank each committee member, Dr. Edmond Bowden and Dr. Morteza Khaledi, for their valuable time and suggestions. I would like to thank my colleagues and friends for their cooperation and for making my stay at the North Carolina State University a memorable one. Finally yet importantly, I would specially like to thank Dr. Xinhui Lou, Qiang Liu and Yongsheng Xiao for their valuable suggestions during my research.

TABLE OF CONTENTS

CHAPTER 4: Studies of Inorganic Thin Film Effect on DIOS-MS Performance

LIST OF TABLES

LIST OF FIGURES

CHAPTER 4: Studies of Inorganic Thin Film Effect on DIOS-MS Performance

LIST OF SCHEMES

Chapter 1

General Introduction and Project Objective

1.1 Introduction

Effective desorption/ionization of analytes adsorbed atop of sample of interest is key in applying desorption/ionization on silicon mass spectrometry in MS imaging applications. The chief goal of this Master thesis is to address this issue and study the implications in DIOS-MS. This introduction will focus on three major concepts: 1) the use of matrix-assisted laser desorption/ionization mass spectrometry (MALDI-MS) as an imaging technique, 2) the needs to replace the conventional organic matrix used in MALDI with porous silicon, and 3) the rationale of using polymers as a spacing material to vary analyte-substrate spacing, with the aims of investigating the spacing effects on DIOS-MS performance.

1.2 Matrix Assisted Laser Desorption Ionization

Hillenkamp and Tanaka are the pioneers and responsible for introducing MALDI technique to macromolecules in 1998. The latter was hence awarded the Nobel Prize in 2002. Since then, thousands of papers have been published on various aspects of the technique such as mechanism studies, sample preparation, and a broad range of applications etc.

Conventional MALDI-MS experiments consist of three major processes: 1) Co-crystallization of analyte-matrix molecule: the analyte solution is mixed with a highly

concentrated matrix solution followed by spotting on a MALDI target (usually stainless steel). The mixture dries and results in co-crystallization of analyte and matrix molecules where analyte molecules are embedded in excess matrix molecules; 2) Laser induced matrix/analyte desorption: a UV laser irradiates co-crystallized matrix/analyte clusters, which induces rapid heating and energy accumulation in the matrix crystals, resulting in rapid local sublimation of matrix molecules that carries analyte molecules into the gas phase; 3) Analyte ionization: proton transfer from the matrix to the analyte produces positively charged analyte ions $[M+H]^+$, though other ionic forms such as sodium adducts and potassium adducts are also present. Scheme 1.1 shows a simplified schematic presentation of the MALDI process. Although the exact MALDI mechanism is still under debate, MALDI has exhibited significant benefits in large molecule analysis, such as soft ionization, high mass window (> 2MDa), and good detection sensitivity. Indeed, it has become one of the most powerful analytical tools in analytical, biological, pharmaceutical, environmental, and material science.

In recent years, MS has been increasingly used in an imaging mode to investigate spatial distributions of different molecular species within biological samples. Among all the MS methods, MALDI is the most widely used imaging mass spectrometry (IMS) source. As shown in Scheme 1.2 in a MALDI-IMS process, a thin slice of tissue sample, usually ~10 μm in thickness, is fixed on a MALDI target plate. The matrix solution is subsequently sprayed or micro-spotted onto the tissue section. The mass spectrum from each discrete x and y position on the sample surface is then obtained that provides an independent molecular profile (i.e. mass, intensity etc.) of thousands of molecules at that

particular location. Thousands of spectra are collected sequentially when the laser rasters across the tissue surface. Plotting the ion intensities of the molecule of interest against the original x, y coordinates generates a 2-D image of that molecule on the sample surface. Due to its structural specificity and multiplexing detection capabilities, in comparison to conventional optical imaging methods, IMS allows scientists to probe and map unknown chemical contents of samples of interest. Additional advantages, such as generic detection of molecules of different classes, relatively simple sample preparation, and label-free detection of analytes in their native forms, make IMS a unique technology over other imaging methodologies.[1-4]

The major concern of MALDI-IMS in practice is the intense background signals of the matrix molecules in the low-mass window ($m/z < 600$), which makes confident identification of small molecules difficult and ultimately limits the applicability of MALDI in detection of low-molecular-weight compounds. Additional concerns of MALDI-IMS include: 1) the difficulty in selection of optimal matrix to allow analysis of different classes of analytes simultaneously with optimal desorption/ionization, and 2) application of the matrix solution to the biological sample, which can cause analyte spatial relocation.

1.3 Surface Assisted Laser Desorption Ionization

Since the first demonstration of using 30 nm cobalt particles suspended in glycerol for detection of large protein molecules by Tanaka *et al*., a variety of nano materials has been examined in surface-assisted laser desorption/ionization-MS (SALDI),

including graphite particles, activated carbon, carbon nanotubes, and metal oxides.[5-13] The major advance in SALDI came in 1999 when Wei *et al.* reported detection of organic compounds utilizing meso-porous (2-50nm) silicon.[14] The technique is known as desorption ionization on porous silicon (DIOS). Attracted by its perspective as an effective matrix-free ionization technique, intense research to study the experimental attributes followed. To date, it has been found that MS spectra can be obtained from DIOS substrate with pores size ranging from 2-200 nm. Reproducible spectra for small molecules achieved from DIOS substrate with pores size of ≈10 nm. In addition, the pore size and the overall porosity of the substrate need to be large enough to support a platform for DIOS-MS.[15] The porous structure of the DIOS substrate is suspected to supply the platform for analyte and solvent molecule retention, whereas the physical properties of the porous surface, such as its optical absorptivity, and thermal conductivity, promotes efficient laser energy absorption and transfer to generate intact analyte ions upon laser irradiation.[14, 16]

Because of simple sample preparation, high salt tolerance, low background noise in lower mass region, and better sensitivity over other SALDI substrates, DIOS-MS has shown potential in numerous applications such as quantitative analysis of low mass species, monitoring enzyme activity and as detectors for chromatographic separations, and lab-on-a-chip technology etc.[17, 18] DIOS based imaging has also been reported that allows mapping of small molecules without background interference providing complementary information to MALDI.[15, 19]

As a surface structure-based analytical method, the molecules in direct contact with the porous Si surface are expected to be the prerequisite of effective detection of any analyte molecules. However, in DIOS-IMS the biological tissues are placed on the top of the porous silicon substrate. Under most experimental conditions, the tissue material is not noticably removed by ablation i.e. only the very top-layer of the tissue sample is sampled. A legitimate concern is thus raised on the effectiveness of DIOS-IMS since the sampling plane is not in direct contact with the porous surface. More specifically, the tissue sample as an insulating spacing layer between the analytes and the porous surface is suspected to impede effective energy transferring during analyte desorption. The drastic difference in the surface chemistry surrounding the analyte molecules atop the substrates with thick tissue to the ones without is also expected to change MS ionization profiles. Therefore, a thorough study on the implication of the presence of an insulating spacing layer on the practicality of DIOS-IMS is imperative.

1.4 Polymer as a spacing material

Biological tissue is composed of mostly non-conducting organic components. However, its chemical complexity and the difficulty in obtaining variable slice thicknesses, opted for make it unrealistic to be used in analyte-substrate spacing studies. In this study, the effect of the spacing distance between the analyte molecules and the porous substrates on DIOS-MS performance was investigated using two organic spacing materials, poly(sodium 4-styrene sulfonate) (PSS) and poly(allylamine hydrochloride) (PAH), to mimic the soft biological tissues of different slicing thicknesses.[20, 21] The

selection of polymer over inorganic films or actual biological tissue samples was made for the following reasons: first, deposition of polymer films has been well-studied in the literature. In particular, spin-coating is routinely used by material scientists to form a uniform, thin layer of organic films on surface.[22, 23] Experimental parameters, such as spin velocity, solution viscosity, and solution volume, have been thoroughly investigated to yield thin films of well-controlled and continuously variable thicknesses. Secondly, the physical properties of polymer films resemble more to those of biological samples than inorganic. The thermal conductivity, optical transparency, and electric resistivity of polymer films are similar to those of animal tissues; thus similar efficacy in molecule desorption and ion extraction is expected.[24, 25] Last but not the least, the relatively simple chemical environment provided by the polymer films compare to that of actual biological samples makes data interpretation straightforward. The ease of altering surface functionality by simply switching to a different polymer system further broadens the capability of investigating the role of surface chemistry in MS measurements.

The focus of the chapter 2 and 3 is to study the impact of analyte-substrate spacing in DIOS-MS imaging. In Chapter 2, analyte-substrate spacing impacts on DIOS-MS performance studied using PSS as the insulating layer and reserpine as the MS standard.

In chapter 3, the spacing effect was further investigated using systems composed of different analytes and the spacing materials to examine the generic applicability of the drawn conclusion from chapter 2. Two analytes of different basicity, 1,2-dipalmitoyl-sn-glycero-3-phosphocholine (DPPC) and ketoprofen, were used as the additional MS

standards. The spacing material of opposite charges, i.e. polyallylamine hydrochloride (PAH), was studied as well.

In Chapter 4, the impacts of thin inorganic film and surface functionality studied. In particular, thin SiOx film obtained via peroxide oxidation. The MS measurements were conducted using reserpine as a standard for varied SiOx film thickness. In later part, MS signal for ketoprofen from different surface (i.e native, oxidized and derivatized) were compared to study the impacts of surface functionality on analyte desorption/ionization efficiency.

1.5 References

1. Drexler, D. M., Garrett, T. J., Cantone, J. L., *et al.*, Utility of imaging mass spectrometry (IMS) by matrix-assisted laser desorption ionization (MALDI) on an ion trap mass spectrometer in the analysis of drugs and metabolites in biological tissues, *Journal of Pharmacological and Toxicological Methods,* (2007), *55,* 279.
2. Chaurand, P., Norris, J. L., Cornett, D. S., *et al.*, New developments in profiling and imaging of proteins from tissue sections by MALDI mass spectrometry, *Journal of Proteome Research,* (2006), *5,* 2889.
3. Cornett, D. S., Reyz'Aer, M. L., Chaurand, P., *et al.*, MALDI imaging mass spectrometry: molecular snapshots of biochemical systems, *Nature Methods,* (2007), *4,* 828.
4. Reyz'Aer, M. L., and Caprioli, R. M., MALDI-MS-based imaging of small molecules and proteins in tissues, *Current Opinion in Chemical Biology,* (2007), *11,* 29.
5. Kinumi, T., Saisu, T., Takayama, M., *et al.*, Matrix-assisted laser desorption/ionization time-of-flight mass spectrometry using an inorganic particle matrix for small molecule analysis, *Journal of Mass Spectrometry,* (2000), *35,* 417.
6. Dale, M. J., Knochenmuss, R., and Zenobi, R., Graphite/Liquid Mixed Matrixes for Laser Desorption/Ionization Mass Spectrometry, *Analytical Chemistry,* (1996), *68,* 3321.

7. Tanaka, K., Waki, H., Ido, Y., *et al.*, Protein and polymer analyses up to m/z 100,000 by laser ionization time-of-flight mass spectrometry, *Rapid Communications in Mass Spectrometry,* (1988), *2,* 151.

8. La, E. P. C., Owega, S., and Kulezycki, R., Time-of-flight mass spectrometry of bioorganic molecules by laser ablation of silver thin film substrates and particles, *Journal of Mass Spectrometry,* (1998), *33,* 554.

9. Sunner, J., Dratz, E., and Chen, Y.-C., Graphite surface-assisted laser desorption/ionization time-of-flight mass spectrometry of peptides and proteins from liquid solutions, *Analytical Chemistry,* (1995), *67,* 4335.

10. Schuerenberg, M., Dreisewerd, K., and Hillenkamp, F., Laser Desorption/Ionization Mass Spectrometry of Peptides and Proteins with Particle Suspension Matrixes, *Analytical Chemistry,* (1999), *71,* 221.

11. Han, M., and Sunner, J., An activated carbon substrate surface for laser desorption mass spectrometry, *Journal of the American Society for Mass Spectrometry,* (2000), *11,* 644.

12. Chen, Y.-C., Shiea, J., and Sunner, J., Thin-layer chromatography-mass spectrometry using activated carbon, surface-assisted laser desorption/ionization, *Journal of Chromatography, A,* (1998), *826,* 77.

13. Xu, S., Li, Y., Zou, H., *et al.*, Carbon nanotubes as assisted matrix for laser desorption/ionization time-of-flight mass spectrometry, *Analytical Chemistry,* (2003), *75,* 6191.

14. Wei, J., Buriak, J. M., and Siuzdak, G., Desorption-ionization mass spectrometry on porous silicon, *Nature,* (1999), *399,* 243.

15. Kruse, R. A., Rubakhin, S. S., Romanova, E. V., *et al.*, Direct assay of Aplysia tissues and cells with laser desorption/ionization mass spectrometry on porous silicon, *Journal of Mass Spectrometry,* (2001), *36,* 1317.

16. Shen, Q., Takahashi, T., and Toyoda, T., Characterization of optical and thermal properties of porous silicon using photoacoustic technique, *Analytical Sciences,* (2001), *17,* S281.

17. Hu, L. G., Xu, S. Y., Pan, C. S., *et al.*, Preparation of a biochip on porous silicon and application for label-free detection of small molecule-protein interactions, *Rapid Communications in Mass Spectrometry,* (2007), *21,* 1277.

18. Shen, Z. X., Thomas, J. J., Averbuj, C., *et al.*, Porous silicon as a versatile platform for laser desorption/ionization mass spectrometry, *Analytical Chemistry,* (2001), *73,* 612.

19. Liu, Q., Guo, Z., and He, L., Mass spectrometry imaging of small molecules using desorption/ionization on silicon, *Analytical Chemistry,* (2007), *79,* 3535.

20. Ma, C., Srinivasan, M. P., Waring, A. J., *et al.*, Supported lipid bilayers lifted from the substrate by layer-by-layer polyion cushions on self-assembled monolayers, *Colloids and Surfaces, B: Biointerfaces,* (2003), *28,* 319.

21. Vidu, R., Zhang, L., Waring, A. J., *et al.*, Phospholipid bilayers on a polyion-alkylthiol layer pair: microprobe imaging, electrochemical properties and peptide

association, *Materials Science & Engineering, B: Solid-State Materials for Advanced Technology,* (2002), *B96,* 199.

22. Denis, F. A., Hanarp, P., Sutherland, D. S., *et al.*, Fabrication of nanostructured polymer surfaces using colloidal lithography and spin-coating, *Nano Letters,* (2002), *2,* 1419.

23. An, M. S., and Hong, J. D., Consecutively spin-assembled layered nanoarchitectures of poly(sodium 4-styrene sulfonate) and poly(allylamine hydrochloride), *Thin Solid Films,* (2006), *500,* 74.

24. Griffith, L. G., Polymeric biomaterials, *Acta Materialia,* (2000), *48,* 263.

25. Hubbell, J. A., Bioactive biomaterials, *Current Opinion in Biotechnology,* (1999), *10,* 123.

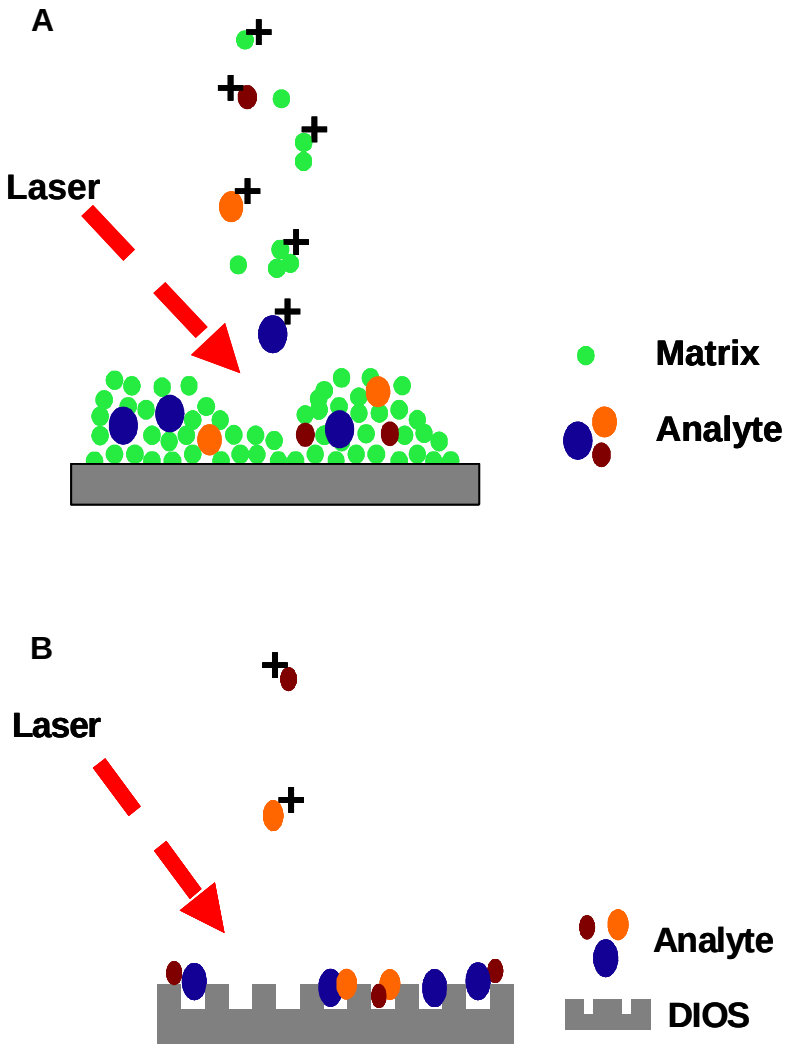

Scheme 1.1 (A, B) Simplified schematic of Matrix-Assisted Laser Desorption/ Ionization (MALDI) and Desorption/ Ionization On porous Silicon (DIOS) process respectively.

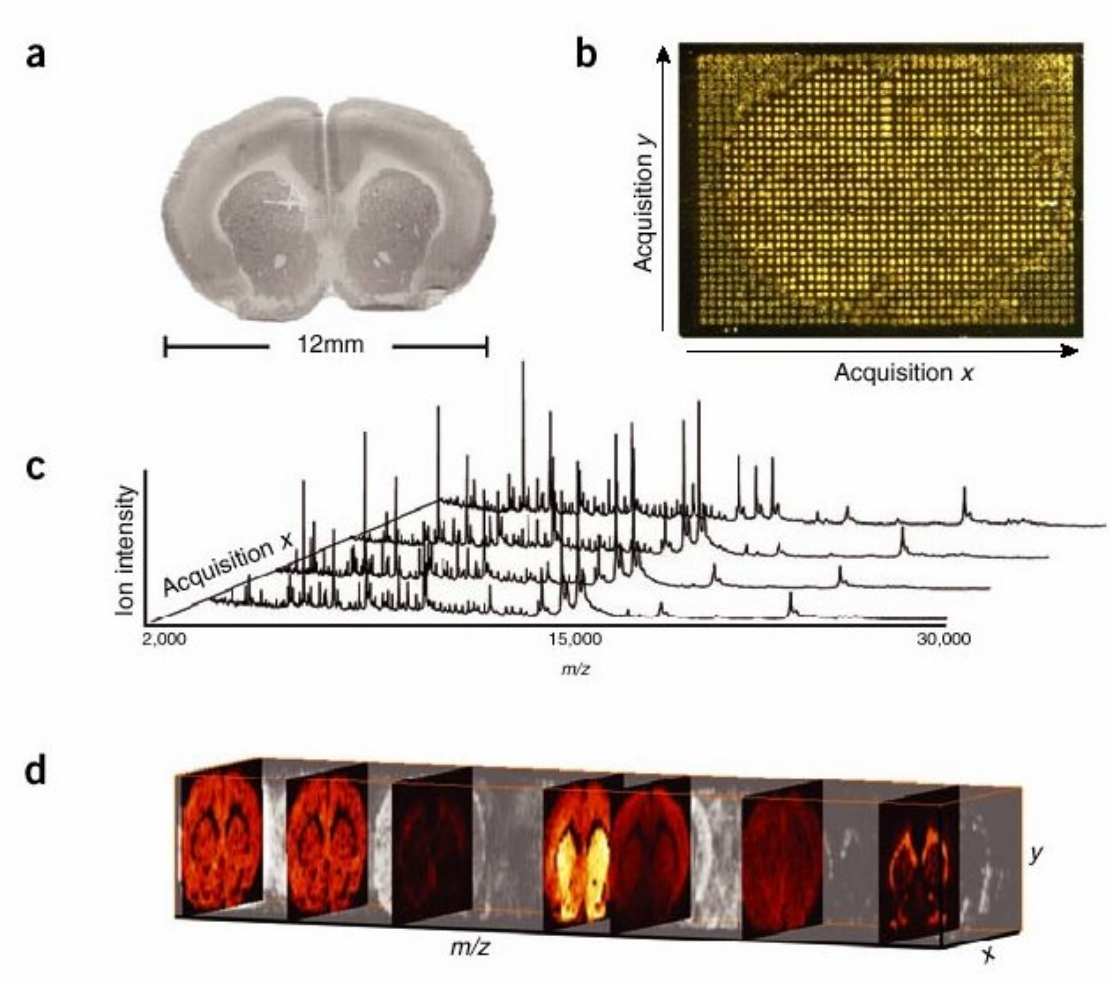

Scheme 1.2 General overview of MALDI-IMS. (a) Fresh section cut from sample tissue (shown here, mouse brain). (b) Mounted section after matrix application using a robotic picoliter volume spotter. (c) Partial series of mass spectra collected along one row of coordinates (x axis). (d) Three-dimensional volumetric plot of complete dataset with selected m/z 'slices' or ion images. Reprinted by permission from Macmillan Publishers Ltd: Nature Methods, **4**(10): p. 828-833, copyright 2007

Chapter 2

Impact of Spacing between Reserpine-DIOS on the Performance of Desorption/ Ionization On porous Silicon Mass Spectrometry (DIOS-MS)

2.1 Introduction

In this chapter, I intend to address questions such as; will analyte-substrate spacing distance effect energy transfer from the substrate to the analyte deposited atop of a polymer layer? If so, what will be the optimal analyte-substrate spacing? Moreover, is there any impact on MS performance due to the change of surface chemistry? How will surface chemistry or analyte properties effect the position of this optimal distance?

In this study, the effect of the spacing distance between the analyte molecules and the porous substrates on DIOS-MS performance was investigated by spin coating synthetic polymer, poly(sodium 4-styrene sulfonate) (PSS), on a porous substrate to mimic the soft biological tissues of different slicing thicknesses.[1, 2] PSS was used as the spacing layer for the following reasons: First, it is easy to deposit, polymer film on the substrate with varied thicknesses of good uniformity and reproducibility. Secondly, given the aromatic structure, PSS is optically transparent at 337 nm, the wavelength at mass spectrometer laser operated. Reserpine, a small drug molecule was used as a MS standard for its neutral property and its solubility in chloroform that allows uniform analyte deposition atop of water-soluble polymer film.

2.2 Experimental

2.2.1 Materials

P-doped (100) single-crystalline silicon wafers of 0.005-0.02 Ω/cm resistivity were purchased from Silicon Sense, Inc. (Nashua, NH) and stored under vacuum until use. Poly (sodium 4-styrene sulfonate) (PSS, M.W.≈ 200,000, 30 wt% in water) was purchased from Sigma Aldrich (St. Louis, MO). (3-Aminopropyl) trimethoxysilane (APTMS, 97%) was purchased from Fluka (St. Louis, MO). Hydrofluoric acid (HF, 49%), hydrogen peroxide (H_2O_2, 30%) and chloroform were purchased from Fisher Scientific (Pittsburgh, PA). Ethanol (CH_3CH_2OH) was purchased from Aaper Alcohol (Shelbyville, KY). DI H_2O of 18 MΩ (Millipore, PO) was used throughout the experiments.

2.2.2 DIOS Substrate Preparation

DIOS substrates were prepared as previously described.[3] Briefly, a Si wafer was cut into 1×1 cm^2 chips, following by dipping into a 5% HF/EtOH solution for 1 min prior to etching to remove the oxidized layer. The chip was electrochemically etched in a 25% HF/EtOH solution for 100 sec at a current density of 5 mA/cm^2 under a 50-W tungsten light. Etched chips were then double etched using a 15% H_2O_2/EtOH solution for 1 minute and stored in 95% EtOH till needed.

2.2.3 Polymer coating on DIOS substrate

Prior to polymer coating, the DIOS substrates were chemically modified: the substrate was first dipped in 15% H_2O_2 /EtOH for 45 minutes, which oxidized the surface and introduced -OH functional groups to the surface. The substrate was then dipped in

50% APTMS/MeOH for 30 minutes to provide a RNH_2- terminated surface. After placing the DIOS substrate on the chuck of the WS-400B-6NPP-LITE spin coater from Laurell technologies, an excess amount (app 2-3 ml) of the PSS solution with known concentration was drop coated on the substrate. The substrate was rotated at high speed (as described in Table 2.1) to spread the solution uniformly on the substrate and to remove any excess solutions. The polymer film thicknesses were measured using an Auto EL Rudolph Ellipsometer. Multiple measurements were taken for each substrate to calculate the average thickness. The substrates were stored in a petri-dish till needed.

2.2.4 MS Measurements

MS analysis was performed on an ABI Voyager DE-STR MALDI-TOF (Applied Biosystems, Foster City, CA) at an accelerating voltage of 20kV in a linear mode. A N_2 laser was used for irradiation. The laser energy was varied to achieve optimal MS performance. MS spectra were acquired by averaging spectra from 5 shots. For each data point, 50-100 spectra were collected from different locations on the same substrate.

Reserpine was dissolved in chloroform with a final concentration of 0.8 mM and used as the standard throughout this study. To deposit the analyte, the substrates with or without polymer coatings were immersed into solution for 1 min and air dried prior to MS analysis to circumvent the nonhomogeneity introduced by analyte drop-coating. Given the solvent evaporation rate, freshly prepared reserpine solution was used for each experiment.

2.2.4 Data analysis

Mass spectra were extracted using an in-house DAT converter software and data were exported to excel spreadsheet. The absolute ion intensities were used directly without spectrum processing to obtain the total ion current (TIC) of reserpine at each laser influx, MS intensities of the molecular ion and its fragment ions were located in the spreadsheet and totaled. The Signal-to-background ratios (S/B) of each ion were calculated using Data Explorer, the built-in software provided by the instrument manufacturer. Final data were plotted using Origin 6.0 (Microcal software, Inc.).

2.3 Result and Discussion

To investigate the spacing effect, PSS (Figure 2.1 A) was used as the spacing material to provide different distances between analyte molecules deposited atop the polymer films and the porous substrate underneath the film (Scheme 2.1). The polymer coating parameters were first optimized on a flat silicon surface and were used to prepare polymer coatings on a DIOS substrate. The Si surfaces were chemically modified prior to spin-coating as described in the experimental section. To cast polymer film, an excess amount of the solution (app 2-3 mL) was first drop-coated on the Si substrate. The substrate was then rotated at high speed to allow the solution to spread uniformly across the surface under centrifugal force. While the rotation continued, the excess solution was spun off the edge of the substrate and it left a uniform film layer on the surface. The thickness of the resulting film was controlled by the original concentration of the solution and the spinning speed, i.e. higher the spinning rate and less viscous the solution led to a

thinner film on the substrate (Table 2.1). Under the optimized depositing conditions, linear correlations between the initial solution concentrations and the final film thicknesses were established for PSS (Figure 2.1B). In most cases, the resulting films were uniform across the surface with less than 10% variation.

To evaluate the effect of the distance between the analyte and the porous substrate on DIOS-MS performance, reserpine was selected as a MS standard molecule for its neutral pKa (6.6) that eliminates possible electrostatic concentrating effect on PSS. Figure 2.2 shows detection of reserpine on DIOS and on a 20-nm PSS-coated DIOS substrate. The molecular ion peak (m/z = 609.6) of reserpine and two small fragments ($[C_{10}H_{12}O_4]^+$, m/z = 196.1 and $[C_{23}H_{30}O_4N_2]^+$, m/z = 398.2) were clearly detected on both surfaces. The relative fragment ion intensities, however, were different where lower relative ion intensities from the fragment ions were observed from the PSS-coated substrate under best signal-to-background condition, regardless a higher laser fluence was used. It is suspected that the insulating surface (i.e. PSS-coated surface) reduced the amount of energy directly deposited into the adsorbed molecules; thus less fragmentation, i.e. "softer" ionization. This speculation was supported by the observation of increased fragmentation under elevated laser irradiation for both substrates. Sodium adducts were observed from both surfaces, but the polymer-coated surface gave rise to more intense alkaline-adduct peaks due to the presence of a higher concentration of Na^+ on the surface as the counter ions in the PSS solution.

Taking into account of different ionic species, the total ion currents (TIC) of reserpine ($TIC = \Sigma I_{[Molecular\ Ion+\ Molecular\ adducts]} + \Sigma I_{[Fragment\ Ions]}$) were used to study the

effect of laser fluences in analyte desorption and ionization atop of polymer-coated surfaces. It was clear in Figure 2.3 that the thicker the polymer coating higher the laser energy was required to reach the similar TIC, suggesting that the polymer film as an insulating layer increased the minimal laser energy needed to generate appreciable ions, probably due to less effective shuttling of the energy absorbed by the porous surface to the analytes adsorbed on top of the polymer layer or less effective ion extraction atop a non-conducting surface. As laser fluences increased, a pseudo-linear increase of TIC was observed with similar linear slopes for the substrates of the polymer thickness less than 150 nm. This is different from the uncoated substrate (i.e. bare DIOS) where the TIC increased at a faster rate.

It is important to note, that in most MS detection, the relative ion current is more important in analyte identification and quantification, however, higher TIC does not necessarily translate to a better MS performance. Figure 2.4A shows that although TICs increased with the increasing laser energy, the calculated signal-to-background (S/B) ratios of the molecular ion of reserpine, i.e. the base peak, on a 45-nm PSS-coated substrate shows an initial increase but soon reached a maximum. With further increase in laser flux, the S/B ratio significantly decreased due to an increasing level of background noise and fragmentation. This experimental result suggests the existence of an optimal amount of irradiation energy to reach the best DIOS–MS performance at any given analyte-surface distance. It is noticed that under the optimal condition, the best S/B values calculated for reserpine deposited on the polymer spacers of different thicknesses were relatively constant (Figure 2.4B). Statistical analysis of the S/B ratios from various

substrates showed negligible difference with a F-value of 2.26 ($F_{critical}$ = 2.44; Table 2.2). This relatively stable S/B ratio across a range of the analyte-surface spacing of 0-150 nm suggests detection effectiveness of reserpine molecule ions is independent of the distance away from the porous substrate. In other words, for any given sample thickness, a set of MS experimental conditions exists to yield comparable MS signals. Under these conditions, the TIC was clearly decreasing with the increasing film thickness, suggesting the accompanying decrease of the background noise level (Figure 2.5).

The elevated energy influx is known to increase the noise level as well as molecular fragmentation. To quantitatively differentiate these two factors in DIOS-MS and to investigate the aforementioned "softer" ionization observed from polymer-cushioned substrates, the surviving yield (SY) % of reserpine molecular ions was quantified using:

$$\text{Survival Yield \%} = \frac{\Sigma\, \text{I}[\text{Molecular Ion} + \text{Molecular Adduct}] \times 100\%}{\Sigma\, \text{I}[\text{Molecular Ion} + \text{Molecular Adduct}] + \Sigma\, \text{I}[\text{Fragment Ion}]}$$

Figure 2.6 shows the calculated SY% of reserpine under the condition to obtain best S/B ratios at each thickness. Relatively low percent of the intact molecular ion were calculated for reserpine detected directly on DIOS (42 ± 5%). Conversely, for molecules adsorbed atop of polymer films the average percentage of intact molecular ions for reserpine were above 74% and slightly higher on thicker films (Figure 2.5).

A possible explanation of such an effect can be attributed to the difference between laser-induced desorption and ionization process in DIOS and in polymer-coated DIOS. In DIOS, the porous silicon absorbs the photon energy upon laser irradiation that causes local temperature increases, which leads to fast vaporization of adsorbates (i.e. analyte, solvent etc.) from the surface. The deep and narrow porous channels in a DIOS substrate imposes a confinement effect that possibly results in a rapid one-dimension expansion of plumes that expels desorbed species into gas phase.[4] The one-dimensional plume and increased background pressure contributes to the higher plume densities in DIOS, leading increased intermolecular interaction in the plume that results in fragmentation of the ions. In polymer-coated DIOS, however, the polymer film shields the porous structure and the top-layer is relatively flat. The resulting plume expands in three dimensions instead, with a much weaker expelling force and more diluted form consequently, an increase in laser irradiation energy in polymer-coated DIOS is required but less structural damage observed.

2.4 Conclusions

A well-controlled and uniform polymer film on the DIOS substrate provides viable alternative to biological tissue to investigate the impacts of different spacing thicknesses on DIOS performance. For reserpine atop PSS, the total ion current of analyte at any given thickness is greatly influenced by the irradiation energy. The intensity decreases in general as the spacing increases. However, the change in signal-to-background values has an inflection point, suggesting the existence of optimal irradiation

energy level to achieve best S/B. A relatively constant S/B values over the tested spacing thickness range (0-150 nm) suggests analyte detection could be independent of the distance away from the porous substrate. The phenomenon is mainly attributed to the improved ionization softness confirmed by an increasing surviving yield of reserpine molecular ion.

2.5 References

1. Ma, C., Srinivasan, M. P., Waring, A. J., *et al.*, Supported lipid bilayers lifted from the substrate by layer-by-layer polyion cushions on self-assembled monolayers, *Colloids and Surfaces, B: Biointerfaces,* (2003), *28,* 319.
2. Vidu, R., Zhang, L., Waring, A. J., *et al.*, Phospholipid bilayers on a polyion-alkylthiol layer pair: microprobe imaging, electrochemical properties and peptide association, *Materials Science & Engineering, B: Solid-State Materials for Advanced Technology,* (2002), *B96,* 199.
3. Finkel, N. H., Prevo, B. G., Velev, O. D., *et al.*, Ordered silicon nanocavity arrays in surface-assisted desorption/ionization mass spectrometry, *Analytical Chemistry,* (2005), *77,* 1088.
4. Alimpiev, S., Nikiforov, S., Karavanskii, V., *et al.*, On the mechanism of laser-induced desorption-ionization of organic compounds from etched silicon and carbon surfaces, *Journal of Chemical Physics,* (2001), *115,* 1891.

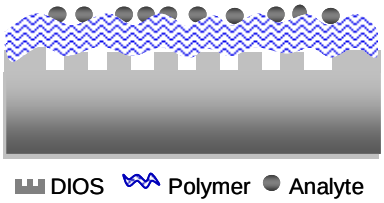

Scheme 2.1 A schematic drawing of analyte-porous surface spacing study using polymer films of tunable thickness.

Table 2.1 The coating parameters used to form PSS films on DIOS.

Concentration (mM)	Spinning Rate (RPM)	Thickness (nm)
0.043	1800	21 +/- 1
0.086	1800	48 +/- 1
0.172	2800	86 +/- 1
0.258	4000	135 +/- 2

Table 2.2 Anova (single factor) performed on signal-to-background data of reserpine detection for each polymer-analyte spacing thickness**.**

Anova: Single Factor

Summary

Groups	Count	Sum	Average	Variance
Column 1	28	631789	22563.89	82388972.91
Column 2	28	710740	25383.57	49110805.81
Column 3	28	686030	24501.07	18563765.25
Column 4	28	624185	22292.32	9572088.60
Column 5	28	600687	21453.11	6685388.17

ANOVA

Source of Variation	SS	df	MS	F	**P-value**	F crit
Between Groups	3.01E+08	4	75133757.7	2.258696987	**0.066041**	2.438739
Within Groups	4.49E+09	135	33264204.1			
Total	4.79E+09	139				

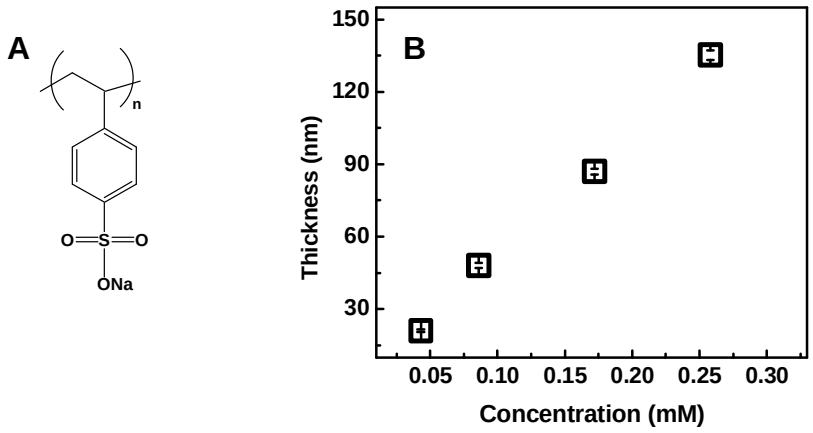

Figure 2.1 Chemical structures of polymer **(A)** poly(sodium-4-styrene sulfonate) (PSS) **(B)** A plot of polymer film thicknesses of PSS on Si after spin-coating as a function of the polymer concentration.

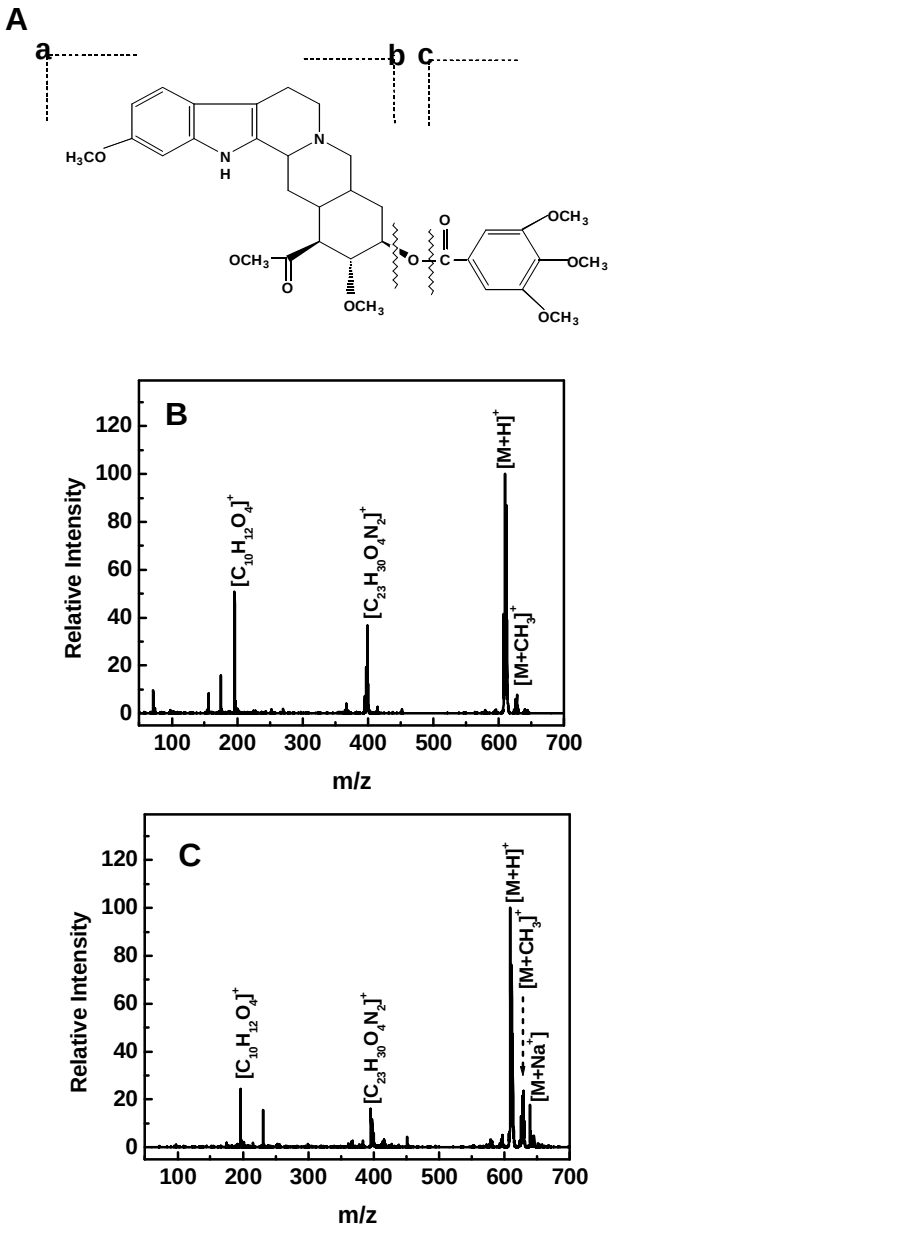

Figure 2.2 **(A)** Chemical structure of Reserpine and the corresponding major fragments. Mass spectra of reserpine detected **(B)** directly on DIOS or atop of PSS-coated DIOS **(C)**. The laser fluxes of 1300 and 1450 (A.U.) were used respectively, the condition to yield the best MS S/B values.

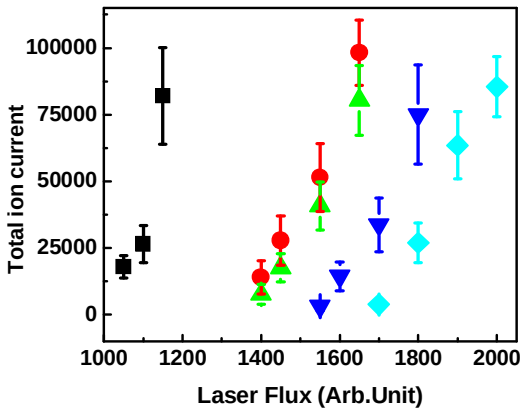

Figure 2.3 A plot of total ion currents of reserpine as a function of varied laser energy for 0 (■), 20 (●), 45 (▲), 90 (▼), and 140-nm (♦) PSS films, respectively.

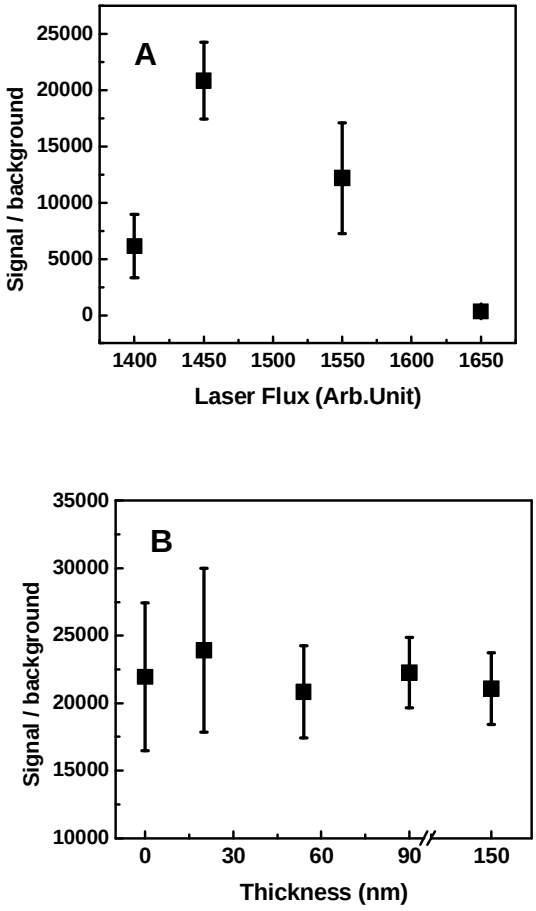

Figure 2.4 **(A)** A plot of the signal/background ratios as a function of the laser flux for DIOS substrates coated with 45-nm PSS. **(B)** Best S/B values obtained for each polymer-analyte spacing thickness.

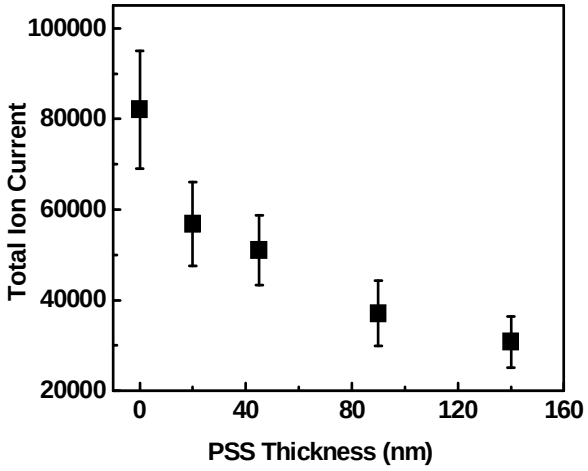

Figure 2.5 Plot of Total ion intensity of reserpine as a function of the PSS thickness for best S/B at each spacing thickness.

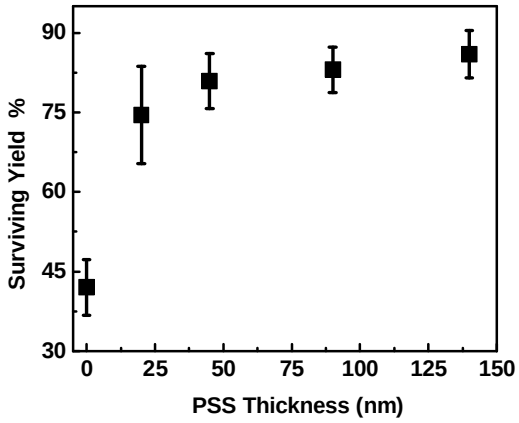

Figure 2.6 Plot of percent of surviving yield of molecular ion as a function of the each analyte-polymer spacing thickness.

Chapter 3

Studies of Analyte-Substrate Spacing Effect on DIOS-MS Performance using Different Analytes and Spacing Materials

3.1 Introduction

It is known that the efficacy of analyte detection in DIOS depends on the properties of the surface functional groups as well as the chemical properties, such as proton affinity (PA) of the analyte to be examined.[1-3] To continuously examine the effect of insulating layers on DIOS-MS and to eliminates analyte specific observations, 1,2-dipalmitoyl-sn-glycero-3-phosphocholine (DPPC) was used as the additional MS standard. In addition, polyallylamine hydrochloride (PAH) was also used in place of PSS to study how a polymer of opposite charge affects MS response. The proton acceptor, primary amine of the PAH, makes analyte detection in positive polarity difficult. Therefore, an acidic molecule ketoprofen was selected as a MS standard to investigate spacing effect using PAH as an insulating layer. When the polymer of opposite charge is used as a spacing material these can exist a concentrating effect of DPPC on PSS or Ketoprofen on PAH due to electrostatic interaction. This can result in more analyte deposition atop polymer layers compare to the bare DIOS. However, the polyelectrolytes charge density is not affected by the varied polymer film thickness. Therefore, in the presence of concentrating effect, comparison between different spacing thicknesses should be comparable to study the spacing effect. In addition, DPPC detection sensitivity experiment allows quantitatively differentiate existence of any concentrating effect.

3.2 Experimental Section

3.2.1 Materials

P-doped (100) single-crystalline silicon wafers at 0.005-0.02 Ω/cm were purchased from Silicon Sense, Inc. (Nashua, NH) and stored under vacuum upon use. 1,2-Dipalmitoyl-*sn*-glycero-3-phosphocholine (DPPC) was purchased from Avanti Polar Lipids, Inc.(Alabaster, AL). Ketoprofen was purchased from MP Biomedicals Inc. (Solon, OH). Poly(sodium 4-styrene sulfonate) (PSS, M.W.≈ 200000,30 wt% in water) was purchased from Sigma Aldrich (St. Louis, MO). Poly (allylamine hydrochloride) (PAH, M.W.≈70000) was purchased from Alfa Aesar (Ward Hill, MA). (3-Aminopropyl)trimethoxysilane (APTMS, 97%) was purchased from Fluka (St. Louis, MO). Hydrofluoric acid (HF, 49%), hydrogen peroxide (H_2O_2, 30%), chloroform and dichloromethane (DCM) were purchased from Fisher Scientific (Pittsburgh, PA). Ethanol (CH_3CH_2OH) was purchased from Aaper Alcohol (Shelbyville, KY). DI H_2O of 18 MΩ (Millipore, PO) was used throughout the experiments.

3.2.2 DIOS Substrate Preparation

DIOS substrates were prepared as previously described.[4] Briefly, a Si wafer was cut into 1×1 cm^2 chips, followed by dipping into a 5% HF/EtOH solution for 1 minute prior to etching to remove the oxidized layer. The chip was electrochemically etched in a 25% HF/EtOH solution for 100 sec at a current density of 5 mA/cm^2 under a 50-W tungsten light. Etched chips were double etched using a 15% H_2O_2/EtOH for 1 min and stored in 95% EtOH till needed.

3.2.3 Polymer coating on DIOS substrate

Prior to polymer coating, the DIOS substrates were chemically modified: the substrate was first dipped in 15% H_2O_2 / EtOH solution for 45 minutes, which oxidized the surface to introduce hydroxyl groups on the surface. The substrate was then dipped in 50% APTMS/MeOH for 30 minutes to provide an amino-terminated surface. In the case of PAH depositions, DIOS substrates with hydroxyl groups were used directly without additional aminosilane modification**.** After placing the DIOS substrate on the chuck of a WS-400B-6NPP-LITE spin coater (Laurell technologies), an excess amount (app 2-3 ml) of polymer solutions with varied concentrations was drop-coated on the substrate. The substrate was rotated at high speed to allow the solution to spread uniformly across the surface and remove any excess solutions. The formed polymer films were measured using an Auto EL, Rudolph Ellipsometer where >3 measurements were taken for each substrate to calculate the average thickness. The substrates were stored without additional drying in a petri-dish till needed.

3.2.4 MS Measurements

MS analysis was performed on an ABI Voyager DE-STR MALDI-TOF (Applied Biosystems, Foster City, CA) at an accelerating voltage of 20kV in a linear mode using a N_2 laser. The laser energy were varied to achieve optimal MS performance. For each data point 50-100 spectra were collected from different locations on the same substrate.

1,2-Dipalmitoyl-*sn*-glycero-3-phosphocholine (DPPC) was dissolved in chloroform with final concentration of 0.7 mM. Ketoprofen was dissolved in

dichloromethane (DCM) with a final concentration of 1.6 mM. These stock solutions were used as the standards throughout this study. Given the solvent evaporation rate, freshly prepared reserpine solution was used for each experiment. To reduce the unhomogeneity introduced by analyte drop-loading, the substrates with and without oxidation were immersed into the selected standard solution for 1 minute and air dried prior to MS analysis to deposit the analyte.

3.2.5 Data analysis

Mass spectra were extracted using an in-house DAT converter software and data were exported to excel spreadsheet. The absolute ion intensities were used directly without spectrum processing to obtain the total ion current (TIC) of reserpine at each laser influx, MS intensities of the molecular ion and its fragment ions were located in the spreadsheet and totaled. The Signal-to-background ratios (S/B) of each ion were calculated using Data Explorer, the built-in software provided by the instrument manufacturer. Final data were plotted using Origin 6.0 (Microcal software, Inc.).

3.3 Result and Discussion

Phosphocholine is one of the most abundant lipids in cell membranes with a natural positive charge in its headgroup. PSS as the spacing material allows stable adsorption of DPPC. Based on literature, neither the charge density nor the polymer film continuity differs significantly at different polymer film thickness. As described in the previous chapter (Table 2.1), the polymer films of different thickness were achievable for PSS on DIOS substrate. In most cases, the resulting films were uniform across the

surface with less than 10% variation in thickness (Figure 3.1C). Figure 3.2 shows the detection of DPPC deposited directly on DIOS and atop of 20-nm PSS-coated DIOS. No molecular ion of DPPC (m/z=734.5) was observed on DIOS due to heavy fragmentation. The spectrum was dominated by two major fragments, $[C_5H_{15}NPO_4]^+$ (m/z=184.1) and $[C_5H_{12}N]^+$ (m/z=86.1). Similarly, despite the observation of the molecular ion as well as its Na^+ adduct, the fragment species were still dominantly present in the spectra from the PSS-coated surfaces. Given that the DPPC fragment ion at m/z=184.1 was most intense with a clean background on both surfaces, it was used to quantitate the spacing effect on DIOS-MS performance in the lower mass region. The MS responses of DPPC at each PSS thickness under varied laser flux were collected.

Similar phenomena were observed as those described in Chapter 2: first, DPPC detection from the PSS-coated substrates required a higher laser flux comparing to the bare DIOS surface to achieve a similar absolute ion intensities, confirming less effective energy transfer to the analyte adsorbed atop the polymer layer (Data not shown). Secondly, the S/B ratios of the major fragment ion exhibited the similar initial increase followed by decrease with the increase in laser irradiation energy, also confirming the existence of optimal irradiation energy to achieve the best S/B values (Figure 3.3A). Last but not the least, the best S/B values of the DPPC fragment ion was relatively unchanged, with a slight decrease at thicker films (Figure 3.3B), the same as the MS responses collected from reserpine atop PSS layers. Statistical analysis of the S/B ratios from various substrates showed no significant difference with a F-value of 2.09, lower than the $F_{critical}$ of 2.84 at 95% confidence level (Table 3.2). This relatively stable S/B ratio across

a range of the analyte-surface spacing confirms detection effectiveness of analyte molecules is less dependent on the distance away from the porous substrate and the charge state of the analytes.

The uncompromised MS performance was also demonstrated in the detection sensitivity measurements of DPPC. A series of DPPC concentrations (100-0.1 μM) were tested on uncoated DIOS and on 45-nm PSS-coated DIOS. Under the conditions where the best S/B values for DPPC fragment ion (m/z=184.1) was achieved from each surface, the measured TIC and S/B values were plotted against the concentration of DPPC (Figure 3.4). The lowest detectable DPPC concentration with S/B values higher than 1000 under the optimized experimental conditions were 0.05 μM (50 fmol/μl) and 0.1 μM (100 fmol/μl) on DIOS and on PSS-coated DIOS surface, respectively. It is worth noting that DPPC molecular ion peak was not observed on DIOS over tested concentration range whereas it was apparent on PSS coated DIOS below 0.5 μM.

To further confirm above results, Poly allylamine hydrochloride (PAH) was used as the spacing material instead of PSS. The sulfonate group of the PSS provides an acidic environment whereas the amine functional groups of PAH provide basic environment. Ketoprofen was used as the MS standard to be detected as $[M-H]^-$ (m/z =253.3). Using the optimized depositing conditions (Table 3.1), the polymer films of different thickness were established for PAH on chemically modified DIOS substrate. The Si-H terminated DIOS surface had an aversion to receive protons which makes ketoprofen detection weak on bare DIOS surface, hence uncoated DIOS surface was derivatized with aminosilane (APTMS) to ensure a similar surface chemical environment. Figure 3.5 shows the

detection of ketoprofen on derivatized DIOS and on a 15-nm PAH-coated surface. The molecular ion peak (m/z = 253.3) of ketoprofen and major fragment ($[C_{15}H_{13}O]^-$, m/z = 209.3) were clearly detected on both surfaces.

The dominant ketoprofen fragment ion (m/z = 209.3) was used to monitor analyte-substrate spacing effect on DIOS-MS performance. Mass spectra were collected under series of laser irradiation for each PAH spacing thickness. The S/B values were calculated for each thickness at varied laser influxes. As observed for PSS-coated surfaces, ketoprofen detection atop of PAH-coated substrate required higher laser influx as the spacing distance increased (i.e. thicker polymer film coating) to generate appreciable ions. Interestingly, Figure 3.6A shows a clear decrease in the optimal S/B values for the ketoprofen fragment ion (m/z=209.3) as the spacer thickness increased, suggesting ineffectiveness of the analyte detection away from the substrate.

The TICs of all three analytes were normalized to the bare DIOS of corresponding analytes. A similar slope for each analyte-polymer pair was observed suggesting that the rate of decrease in TIC as the insulting film thickness increase are very similar to each other (Figure 3.6B). To further investigate the decrease in S/B value the mass spectra of the ketoprofen atop of 60nm PAH coated DIOS and mass spectra of 60nm PAH-coated DIOS without ketoprofen under same instrument condition were compared (figure 3.7). The higher laser influxes for analyte desorption/ionization from thicker film escalated PAH desorption/ionization from DIOS surface. As a result, higher background noise was observed and consequently a decrease in S/B as PAH-coating thickness increased.

3.4 Conclusions

In summary, the analyte-surface spacing effect in DIOS-MS performance was further investigated using DPPC and ketoprofen as MS standards and PSS and PAH as the insulating materials. The results conclude: 1) an increase in the laser threshold is needed to generate appreciable ions probably due to ineffectiveness of energy transfer from porous silicon to the analyte deposited atop insulated layer; 2) reduced TIC was collected as the analyte-substrate distance increase and the decreasing slope is independent of the analyte studied; 3) the signal-to-background values are insensitive to the analyte-substrate spacing in the case of DPPC but decrease significantly in ketoprofen due to PAH fragmentation.

3.5 References

1. Alimpiev, S., Grechnikov, A., Sunner, J., *et al.*, On the role of defects and surface chemistry for surface-assisted laser desorption ionization from silicon, *Journal of Chemical Physics,* (2008), *128*.
2. Liu, Q., and He, L., Quantitative Study of Solvent and Surface Effects on Analyte Ionization in Desorption Ionization on Silicon (DIOS) Mass Spectrometry, *Journal of the American Society for Mass Spectrometry,* (2008), *19,* 8.
3. Trauger, S. A., Go, E. P., Shen, Z. X., *et al.*, High sensitivity and analyte capture with desorption/ionization mass spectrometry on silylated porous silicon, *Analytical Chemistry,* (2004), *76,* 4484.
4. Finkel, N. H., Prevo, B. G., Velev, O. D., *et al.*, Ordered silicon nanocavity arrays in surface-assisted desorption/ionization mass spectrometry, *Analytical Chemistry,* (2005), *77,* 1088.

Table 3.1 The coating parameter used to form PAH film on DIOS.

	Concentration (mM)	Spinning Rate (RPM)	Thickness (nm)
PAH	0.08	3400	14 ± 1
	0.16	3400	28 ± 1
	0.25	4200	52 ± 1.5

Table 3.2 Anova (single factor) performed on signal-to-background data of DPPC detection for each polymer-analyte spacing thickness**.**

Anova: Single Factor						
Summary						
Groups	Count	Sum	Average	Variance		
Column 1	11	256400.8	23309.1591	16654754		
Column 2	11	260400.8	23672.7955	13383572		
Column 3	11	236151.3	21468.2955	6169861.7		
Column 4	11	225618.3	20510.7576	11348124		
ANOVA						
Source of Variation	SS	df	MS	F	**P-value**	F crit
Between Groups	74599921	3	24866640.3	2.0915533	**0.116587**	2.838746
Within Groups	4.76E+08	40	11889078			
Total	5.5E+08	43				

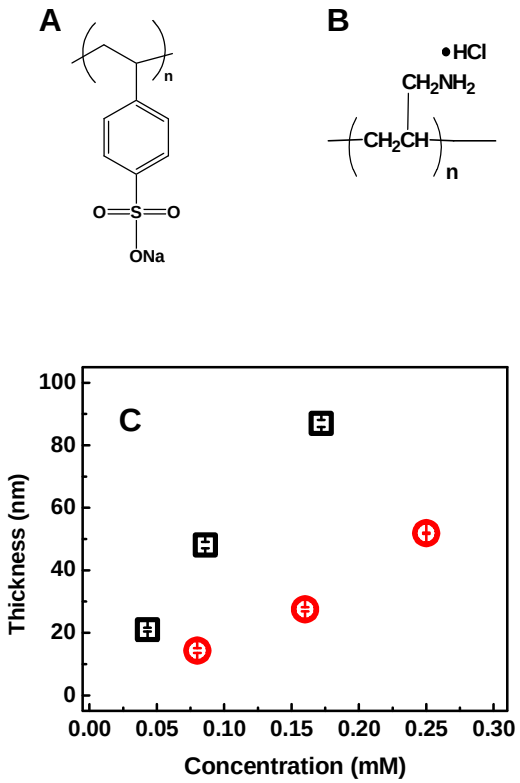

Figure 3.1 Chemical structures of (A) poly(sodium-4-styrene sulfonate) (PSS) (B) poly(allylamine hydrochloride) (PAH). (C) A plot of polymer film thicknesses of PSS (□) and PAH (○) on Si after spin-coating as a function of the polymer concentration.

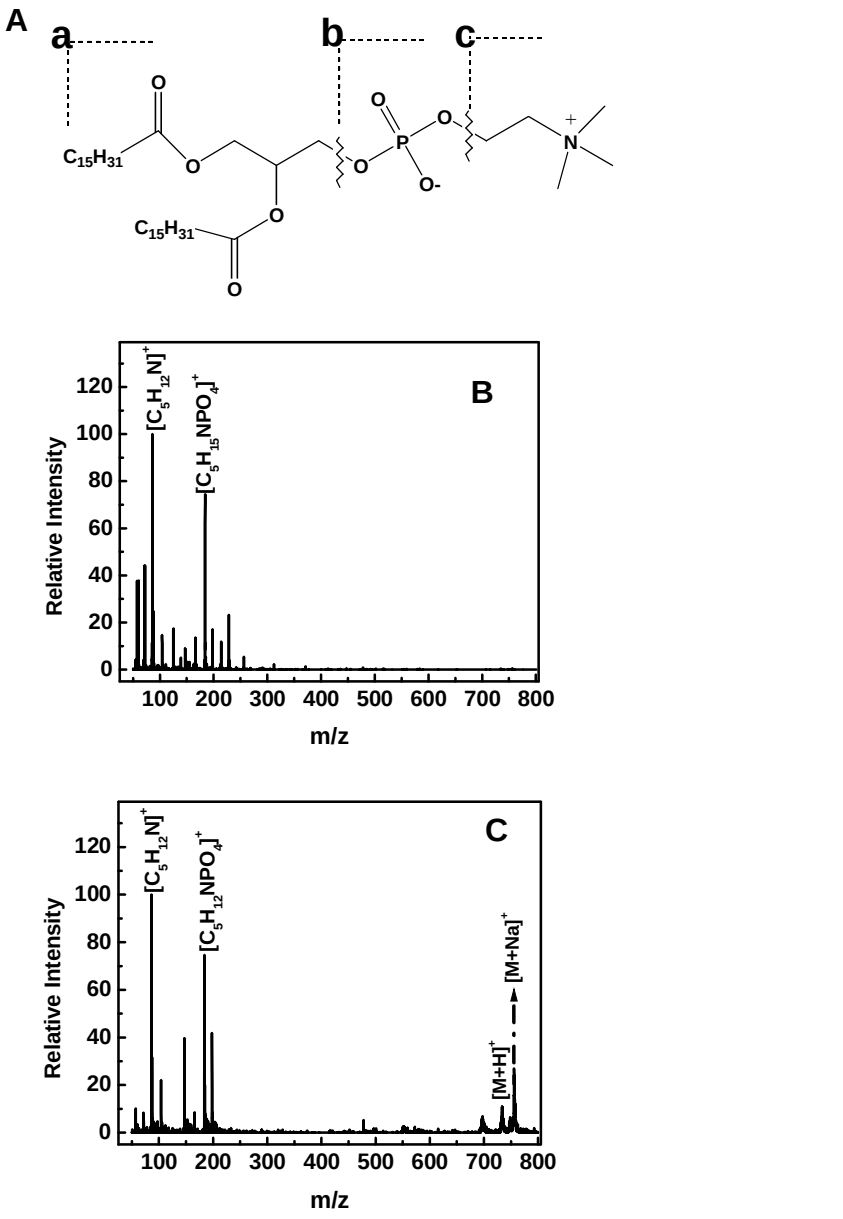

Figure 3.2 (A) Chemical structure of DPPC and the corresponding major fragments. Mass spectra of DPPC detected (B) directly on DIOS and (C) atop of 20 nm PSS-coated DIOS. MS spectra collected under following instrument conditions: 1300 and 1750 laser fluence (a.u.) respectively, 0.7 mM DPPC solution and 5 laser shots/spectrum etc.

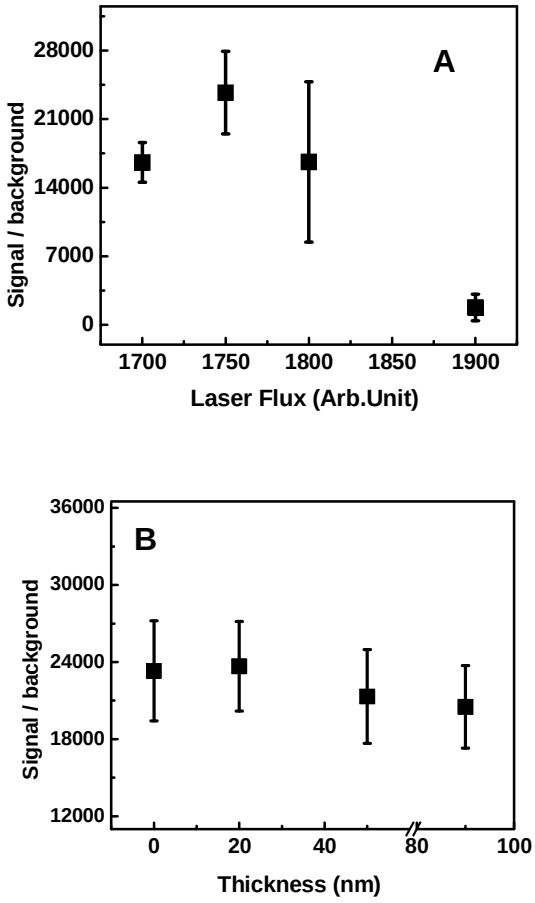

Figure 3.3 (A) A plot of the signal-to-background ratios as a function of the laser fluences for DIOS substrates coated with 20-nm PSS. (B) Highest S/B values obtained for each polymer-analyte spacing thickness for DPPC atop of PSS.

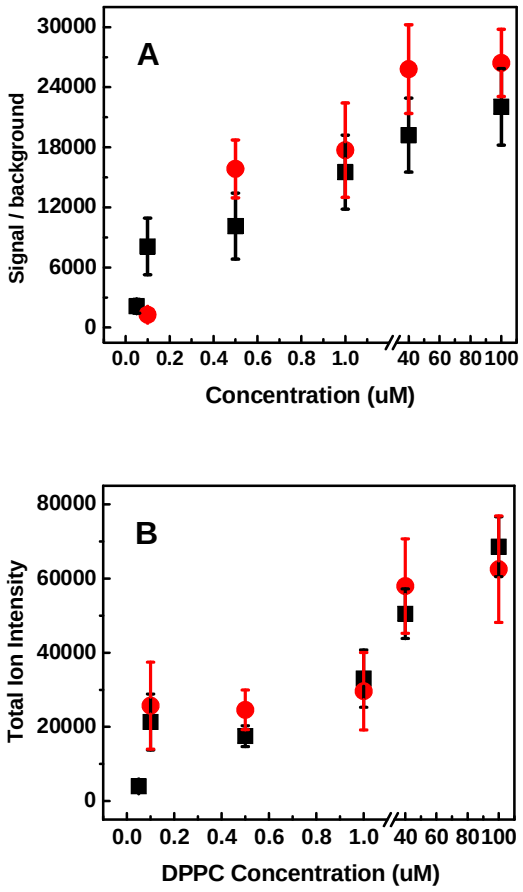

Figure 3.4 (A, B) Plot of highest S/B and total ion current of DPPC at S/B as a function of DPPC concentration on DIOS(■) and on 45nm PSS(●) coated DIOS respectively.

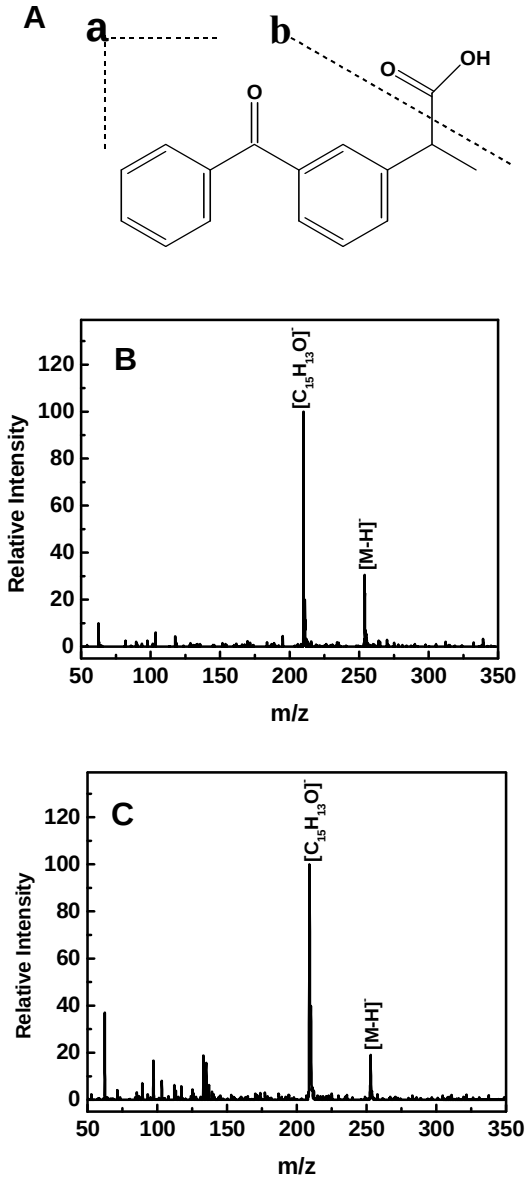

Figure 3.5 (A) Chemical structure of ketoprofen and the corresponding major fragment. Mass spectra of ketoprofen detected (B) directly on derivatized DIOS and (C) atop of 15 nm PAH-coated DIOS.

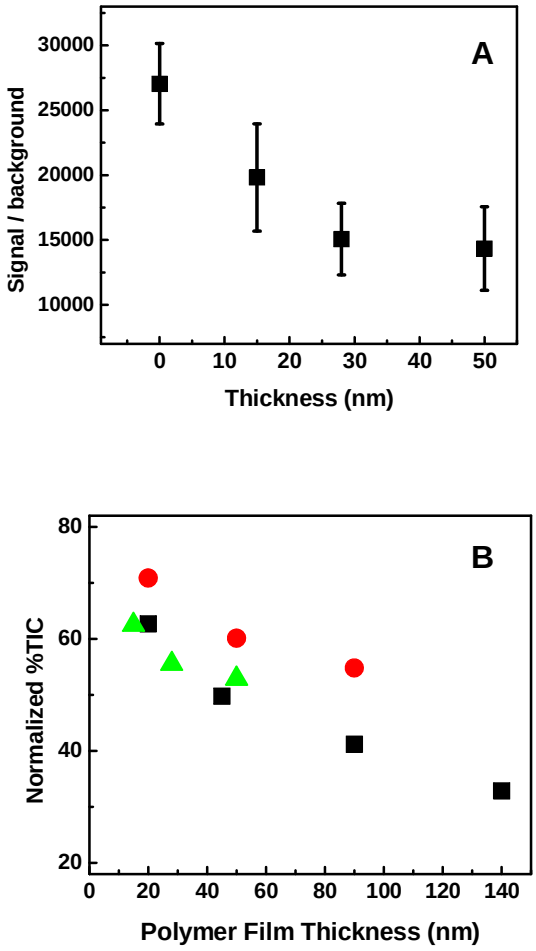

Figure 3.6 **(A)** The highest S/B values obtained for each PAH polymer-analyte spacing thickness for ketoprofen fragment ion (m/z=209.3). (B) Plot of normalized total ion currents of reserpine (■), DPPC (●) and ketoprofen (▲) as a function of the PSS or PAH thickness for best S/B at each spacing thickness.

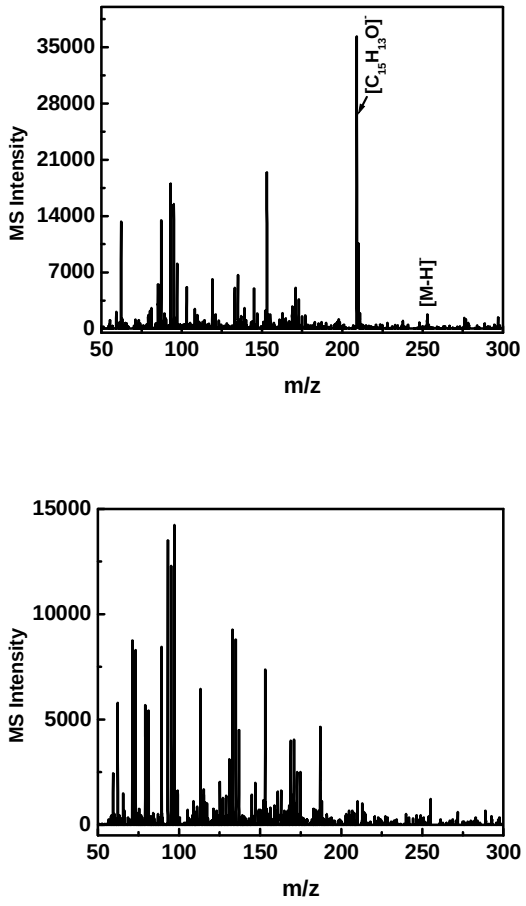

Figure 3.7 (A) Mass spectra of ketoprofen detected atop of 60nm PAH-coated DIOS (B) Mass spectra from 60nm PAH coated DIOS surface without analytes under the same instrument condition.

Chapter 4

Studies of Inorganic Thin Film Effect on DIOS-MS Performance

4.1 Introduction

The introduction of surface-based desorption/ionization technology has allowed analysis of small molecules.[1-3] The most prominent example of SALDI-MS approaches was reported by Suizdak et al, known as Desorption/Ionization On porous Silicon (DIOS) in which porous silicon (pSi) is utilized as SALDI substrate.[2-4] Although the DIOS mechanism is not entirely understood, preliminary investigation suggests porous silicon morphology such as the pore size, porosity of the substrate, porous layer thickness, etc. play vital role in DIOS performance.[3, 5, 6] However, as mentioned in literature, the porous silicon surface is susceptible to oxidation, from exposure to air, to ozone, or to peroxide solutions.[7-9] Oxidation of porous silicon is commonly suspected and has been reported to have detrimental effect on DIOS performance due to changes in the chemical and physical properties of the substrates. For example, the hydrophobic porous Si after etching, changed to rapidly hydrophilic upon oxidation. Consequently, the loss of analyte confinement in the small area occurs when the analyte was in an aqueous solution. Oxidation of the porous silicon also causes migration of the analyte and consequently results in low MS signal when compared with freshly etched surface.[3] In addition, the growth of a thin layer of SiO_2 film makes pores smaller that decreases the overall porosity and changes the thermal conductivity of the substrate by introducing an

insulating layer.[10] However, there is no detailed knowledge about how ultra-thin SiOx film affect DIOS measurements.

In contrast, Gorecka-Drzazga *et al.* have reported that porous silicon dioxide is viable for analysis of small molecules (desorption/ionization on porous silicon dioxide (DIOSD). The advantages listed for DIOSD over DIOS, are high chemical passivity, simpler substrate fabrication and higher signal-to-noise.[11] Similarly, Vaidyanathan and co-workers compared the usefulness of oxidized and unoxidized DIOS surfaces in detection of protonated/deprotonated compounds.[12] Oxidation of the pSi results in change of surface wettability and subsequently analyte-surface interaction. Nevertheless, the discrepancy between two drastically different observations in oxidized pSi was not explained and is still not well understood.

Here, I investigated the impact of inorganic materials (i.e. SiOx film) on DIOS-MS measurements. In particular, DIOS substrates were oxidized for different time intervals with peroxide to obtain varied thickness of SiOx film. DPPC and Reserpine were used as MS standards, total ion currents (TIC) of the analytes detected on varied SiOx film thickness compared. Signal-to-background (S/B) ratios and survival yields (SY) of the reserpine molecular ion were used to further quantitate the impact of the SiOx film thickness on DIOS-MS performance.

In addition, chemical modification of the porous silicon was also studied. Silane molecules have been routinely used in the literature to improve detection sensitivity and specificity of the analyte molecules. Derivatization of the porous silicon not only alters the surface chemical properties but also improves surface stability against oxidation and

hydrolysis that retains the DIOS-MS activity for an extended period.[13] The ease of altering SiOx functionality by simply running silane chemistry with different molecules further broadens the capability to investigate the role of different surface functionality in the desorption/ionization process in DIOS. In this study, Ketoprofen was used as the MS standard to compare the change in MS signal due to the change in surface functionality.

4.2 Experimental Section

4.2.1 Materials

P-doped (100) single-crystalline silicon wafers at 0.005-0.02 Ω/cm resistivity were purchased from Silicon Sense, Inc. (Nashua, NH) and stored under vacuum upon use. 1,2-Dipalmitoyl-sn-glycero-3-phosphocholine (DPPC) was purchased from Avanti Polar Lipids, Inc.(Alabaster, AL). Ketoprofen was purchased from MP Biomedicals Inc. (Solon, OH). Reserpine was purchased from Sigma Aldrich (St. Louis, MO). (3-Aminopropyl)trimethoxysilane (APTMS, 97%) was purchased from Fluka (St. Louis, MO). Hydrofluoric acid (HF, 49%), hydrogen peroxide (H_2O_2, 30%) and chloroform were purchased from Fisher Scientific (Pittsburgh, PA). Ethanol (CH_3CH_2OH) was purchased from Aaper Alcohol (Shelbyville, KY). DI H_2O of 18 MΩ (Millipore, PO) was used throughout the experiments.

4.2.2 DIOS Substrate Preparation

DIOS substrates were prepared as previously described[14]. Briefly, a Si wafer was cut into 1×1 cm^2 chips, following by dipping into a 5% HF/EtOH solution for 1 min prior to etching to remove the oxidized layer. The chip was electrochemically etched in a 25%

HF/EtOH solution for 100 sec at a current density of 5 mA/cm^2 under a 50-W tungsten light. Etched chips were double etched using a 15% H_2O_2/EtOH for 1 min and stored in 95% EtOH till needed.

To generate different thickness of the SiOx film on DIOS surface, substrates immersed in 15% H_2O_2 / EtOH for different time intervals at room temperature that oxidized the surface and introduced -OH functional groups to the surface. The SiOx film thickness measured using an Auto EL, Rudolph Ellipsometer where multiple measurements taken for each substrate to calculate the average thickness. The substrates were stored in EtOH till needed.

To obtain –NH_2 functionality the DIOS substrates were first immersed in 15% H_2O_2 / EtOH for 45 minutes followed by immersion in 50% APTMS/MeOH for 30 minutes to provide a RNH_2 terminated surface.

4.2.3 MS Measurements.

MS analysis performed on an ABI Voyager DE-STR MALDI-TOF (Applied Biosystems, Foster City, CA) at an accelerating voltage of 20kV in a linear mode using a Nitrogen laser. The laser energy were varied to achieve optimal MS performance. For each data point, 50-100 spectra collected from different locations on the same substrate.

1,2-Dipalmitoyl-*sn*-glycero-3-phosphocholine (DPPC) and Reserpine were dissolved in chloroform with final concentrations of 0.7 mM and 0.8 mM, respectively. Ketoprofen was dissolved in dichloromethane (DCM) with a final concentration of 1.6 mM. These stock solutions were used as the standards throughout this study. Due to the fast evaporation of chloroform, freshly prepared reserpine solution was used for each

experiment. To reduce the unhomogeneity introduced by analyte drop loading, the substrates with and without oxidation were immersed into the selected standard solution for 1 min and air dried prior to MS analysis to deposit the analyte.

4.2.4 Data analysis

Mass spectra were extracted using an in-house DAT converter software and data were exported to excel spreadsheet. The absolute ion intensities were used directly without spectrum processing to obtain the total ion current (TIC) of reserpine at each laser influx, MS intensities of the molecular ion and its fragment ions were located in the spreadsheet and totaled. The Signal-to-background ratios (S/B) of each ion were calculated using Data Explorer, the built-in software provided by the instrument manufacturer. Final data were plotted using Origin 6.0 (Microcal software, Inc.).

4.3 Result and Discussion.

The objective of this study was to investigate the impacts of inorganic thin SiOx thickness as well as different chemical environment on analyte desorption/ionization. Specifically, bare DIOS (i.e. freshly HF washed), oxidized DIOS, and chemically derivatized DIOS substrates were used to examine the issue. Scheme 4.1 illustrates the concept of silicon surface oxidation and derivatization. To obtain SiOx film of varied thicknesses on porous silicon surface, DIOS substrates were immersed in 15% hydrogen peroxide solution for different time intervals, which introduce not only –OH functional groups but also provides SiOx film with varied thicknesses to study its impact on DIOS

measurements. The ellipsometric thickness measurements confirmed uniform SiOx film across the surface (Table 4.1).

To evaluate the effect of the SiOx film thickness on DIOS-MS performance, 1, 2-dipalmitoyl-sn-glycero-3-phosphocholine (DPPC) was used the MS standard. Figure 4.1 shows detection of DPPC deposited on bare DIOS and on an oxidized DIOS surface (45 minutes), respectively. The molecular ion (m/z=734.5) as well as its Na^+ adduct were evident. Two fragments, $[C_5H_{15}NPO_4]^+$ (m/z=184.1) and $[C_5H_{12}N]^+$ (m/z=86.1) were also observed on oxidized DIOS surface. Conversely, no molecular ion were observed on bare DIOS and the spectrum was dominated by two major fragment ions. To reduce fragmentation, the MS signals at each SiOx film thickness were collected under the instrumental condition optimized for bare DIOS (i.e. no oxidation). An MS signal collected under the same condition allows direct comparison of the impact of SiOx film thickness on the DIOS-MS performance. The results showed a slight increase in MS intensity of the molecular ion as the SiOx film thickness increases followed by slow decline later, albeit it was still higher than that from bare DIOS (Figure 4.2). The MS intensity of the fragment ion m/z 184.1 as well as the total ion current (TIC) showed slow decline over the tested SiOx film thickness. The MS intensity of the fragment ion (m/z 86.1) was relatively consistent across the tested range. Together, the oxidized porous silicon surface showed slight improvement in molecular ion detection, but a slight decrease in overall ion intensities.

The impact of SiOx film thickness was further investigated using reserpine as a MS standard molecule. Figure 4.3 shows detection of reserpine on DIOS and on oxidized

DIOS substrate. The molecular ion m/z = 609.6 with two small fragments, $[C_{10}H_{12}O_4]^+$, m/z = 196.1 and $[C_{23}H_{30}O_4N_2]^+$, m/z = 398.2, were clearly detected on both surfaces. However, the relative fragment ion intensities were different, in which much lower fragment ion intensities and better S/B ratios were observed from the oxidized substrate. The efficient proton donating capability and better wettability of the acidic surface (i.e. oxidized porous silicon) could be the contributing factor for improved reserpine detection on oxidized surfaces. Sodium adducts were observed from both surfaces; but the oxidized surface gave rise to more intense alkaline-adduct peaks.

Given that different ionic species, the total ion currents (TIC) of reserpine were used to study the effect of laser fluences in analyte desorption and ionization on SiOx surfaces. In LDI-MS the TIC of the analytes greatly depends on the laser irradiation energy. Similar phenomenon was observed from the SiOx films of different thicknesses. It was expected that higher laser irradiation energy was required for thicker SiOx films to reach the similar TIC, suggests shifting of irradiating energy level to generate appreciable ion after certain SiOx film thickness, due to the increased thermal conduction by SiOx film. Surprisingly, less energy was needed to reach similar TIC until the SiOx film nearly 4 nm (Figure 4.4).

As previously has observed, a higher TIC does not necessarily translate to a better MS performance. The signal-to-background (S/B) ratios of reserpine molecular ion (i.e. the base peak) were calculated for each SiOx film thickness similar to polymer-coated surfaces, the experimental results suggests existence of an optimal amount of irradiation energy to reach the best DIOS–MS performance on bare DIOS. The oxidized surfaces

however, showed an increase in the S/B values as the laser reached the upper limit of instrument. Figure 4.5 shows the highest calculated S/B values for reserpine atop of SiOx films of different thicknesses. The much higher S/B ratios across the oxidized substrates suggest lower background interference and high percent of intact molecular ions detected on the oxidized surface than on bare DIOS. The absolute ion intensity were also much higher, as shown in Figure 4.5B.

To understand molecular fragmentation as a function of elevated laser irradiation energy and to quantitatively investigate the "softer" ionization from the oxidized substrates, the surviving yield (SY) % of reserpine molecular ions was quantified using:

$$\text{Survival Yield}\,\% = \frac{\Sigma\, \text{I}\,[\text{Molecular Ion} + \text{Molecular Adduct}] \times 100\%}{\Sigma\, \text{I}\,[\text{Molecular Ion} + \text{Molecular Adduct}] + \Sigma\, \text{I}\,[\text{Fragment Ion}]}$$

Figure 4.6 shows the calculated SY% of reserpine under best S/B ratio condition for each SiOx film thickness. A relatively low percentage of intact molecular ions was calculated for reserpine detected on bare DIOS (42 ± 5%). Conversely, reserpine detection on oxidized surface showed much higher survival yields of molecular ion (> 90%). However, there was not significant impact on survival yield due to the change in SiOx film thickness. The plausible cause for the improved DIOS-MS performance upon surface oxidation can be due to change in surface conductivity or wetting or both. Studies have shown the thermal conductivity of the bulk silicon drops to 1.2 W/m·K from 150 W/m·K after anodic etching to porous structure. However, the conductivity of the SiO_2

given in literature is ~1.4 W/m·K, slightly higher than that of porous silicon. Thus, the change in thermal conductivity due to the oxidation of the surface is probably minimal and falls within experimental deviation. Rather, introduction of –OH on the surface makes it more hydrophilic, which increases the surface acidity. In addition, the increased surface wettability increases the amount of solution inside of small cavities, which could lead to better heat transfer efficiency and more desorption of analyte molecules from fast evaporation through narrow pores.

The speculation was supported by the set of experiments where surfaces of different functionality; Si-H (bare DIOS), Si-OH (oxidized-DIOS) and Si-RNH_2 (derivatized-DIOS) were used to probe the importance of surface functionality (pKa) of the substrate in analyte ionization. Ketoprofen were used as MS model detected under negative polarity as $[M-H]^-$ (m/z =253.3). The change in ketoprofen ion intensity was used to evaluate the contribution from different surface function groups. Figure 4.7 shows the detection of ketoprofen on different surfaces, DIOS, oxidized DIOS and APTMS derivatized DIOS. The Si-H terminated DIOS surface has an aversion to receive proton, which makes ketoprofen detection less effective from the DIOS surface directly. In contrast, primary amine with a lone pair electron, which has an appetite to accept protons, makes ketoprofen detection on derivatized surface more efficient (Figure 4.7D). As shown in spectrum, ketoprofen detection was improved >20 times, comparing Si-H to Si-NH_2. Among the three surface tested, Si-NH_2 is the most basic one followed by Si-H and Si-OH. The logical order for ketoprofen detection in negative polarity should be Si-NH_2 > Si-H > Si-OH. However, surface oxidation changes the surface wettability from

hydrophobic to hydrophilic. The higher wettability (i.e. Hydrophilic surface) led to penetration of the analyte and solvent residues deep inside the porous structure compare to Si-H, which resulted in improved desorption in the plume upon laser irradiation.

4.4 Conclusions

It is described here, an observation of SiOx film and different chemical functional group effect on DIOS-MS performance. The SiOx film on the porous silicon was obtained via peroxide oxidation. Comparing the ionization efficiency in the DIOS and oxidized DIOS revealed an increase in relative intensities of DPPC molecular ion on the SiOx film than DIOS surface. In case of reserpine as a MS model, TIC showed laser irradiation energy dependent monotonic increase. Relatively constant and much higher S/B ratios from SiOx substrate confirmed, analyte detection independent of SiOx film thickness over the tested range. However, It is important to note that oxidized surface gave much higher S/B ratio, low background interference and much higher surviving yield of the molecular ion. Indeed, much better DIOS-MS performance than bare DIOS. Importance of the surface chemical functionality of the DIOS substrate found to play major role for analyte detectability confirmed by the improved ketoprofen detection on basic surface (i.e. derivatized).

4.5 References

1. Go, E. P., Prenni, J. E., Wei, J., *et al.*, Desorption/ionization on silicon time-of-flight/time-of-flight mass spectrometry, *Analytical Chemistry,* (2003), *75,* 2504.
2. Shen, Z. X., Thomas, J. J., Averbuj, C., *et al.*, Porous silicon as a versatile platform for laser desorption/ionization mass spectrometry, *Analytical Chemistry,* (2001), *73,* 612.
3. Lewis, W. G., Shen, Z. X., Finn, M. G., *et al.*, Desorption/ionization on silicon (DIOS) mass spectrometry: background and applications, *International Journal of Mass Spectrometry,* (2003), *226,* 107.
4. Wei, J., Buriak, J. M., and Siuzdak, G., Desorption-ionization mass spectrometry on porous silicon, *Nature,* (1999), *399,* 243.
5. Kruse, R. A., Li, X. L., Bohn, P. W., *et al.*, Experimental factors controlling analyte ion generation in laser desorption/ionization mass spectrometry on porous silicon, *Analytical Chemistry,* (2001), *73,* 3639.
6. Alimpiev, S., Nikiforov, S., Karavanskii, V., *et al.*, On the mechanism of laser-induced desorption-ionization of organic compounds from etched silicon and carbon surfaces, *Journal of Chemical Physics,* (2001), *115,* 1891.
7. Petrova, E. A., Bogoslovskaya, K. N., Balagurov, L. A., *et al.*, Room temperature oxidation of porous silicon in air, *Materials Science and Engineering B-Solid State Materials for Advanced Technology,* (2000), *69,* 152.

8. Thompson, W. H., Yamani, Z., Hassan, L. H. A., *et al.*, Room temperature oxidation enhancement of porous Si(001) using ultraviolet-ozone exposure, *Journal of Applied Physics,* (1996), *80,* 5415.

9. Frotscher, U., Rossow, U., Ebert, M., *et al.*, Investigation of different oxidation processes for porous silicon studied by spectroscopic ellipsometry, *Thin Solid Films,* (1996), *276,* 36.

10. Pirasteh, P., Charrier, J., Soltani, A., *et al.*, The effect of oxidation on physical properties of porous silicon layers for optical applications, *Applied Surface Science,* (2006), *253,* 1999.

11. Gorecka-Drzazga, A., Bargiel, S., Walczak, R., *et al.*, Desorption/ionization mass spectrometry on porous silicon dioxide, *Sensors and Actuators B-Chemical,* (2004), *103,* 206.

12. Vaidyanathan, S., Jones, D., Ellis, J., *et al.*, Laser desorption/ionization mass spectrometry on porous silicon for metabolome analyses: influence of surface oxidation, *Rapid Communications in Mass Spectrometry,* (2007), *21,* 2157.

13. Trauger, S. A., Go, E. P., Shen, Z. X., *et al.*, High sensitivity and analyte capture with desorption/ionization mass spectrometry on silylated porous silicon, *Analytical Chemistry,* (2004), *76,* 4484.

14. Finkel, N. H., Prevo, B. G., Velev, O. D., *et al.*, Ordered silicon nanocavity arrays in surface-assisted desorption/ionization mass spectrometry, *Analytical Chemistry,* (2005), *77,* 1088.

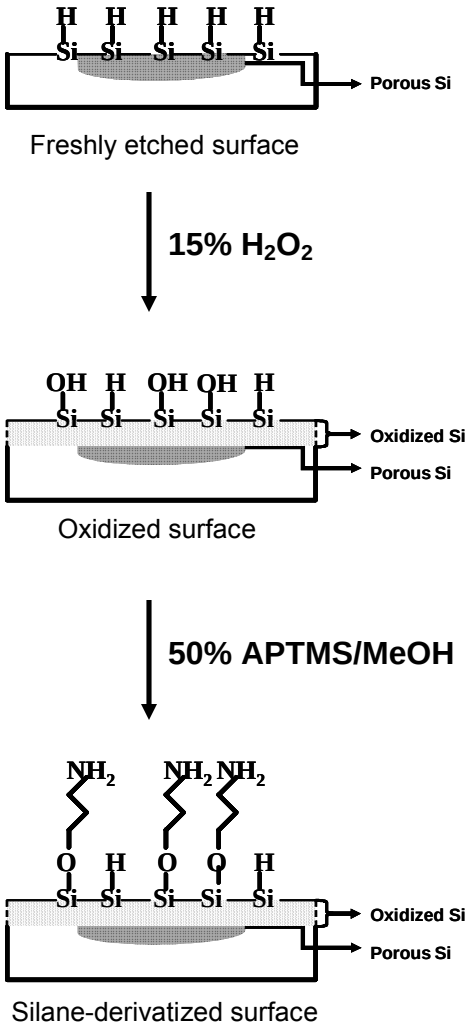

Scheme 4.1 A schematic presentation of DIOS surface oxidation and derivatization by peroxide and APTMS, respectively.

Table 4.1 SiOx film on DIOS surface, the time for DIOS substrate immersed in peroxide solution and resulting SiOx film thickness.

Time (min)	SiOx film Thickness (Å)
10 min	19 +/- 0.5
30 min	23 +/- 1
45 min	27 +/- 1
60 min	30 +/- 1
90 min	35 +/- 1
120 min	39 +/- 1

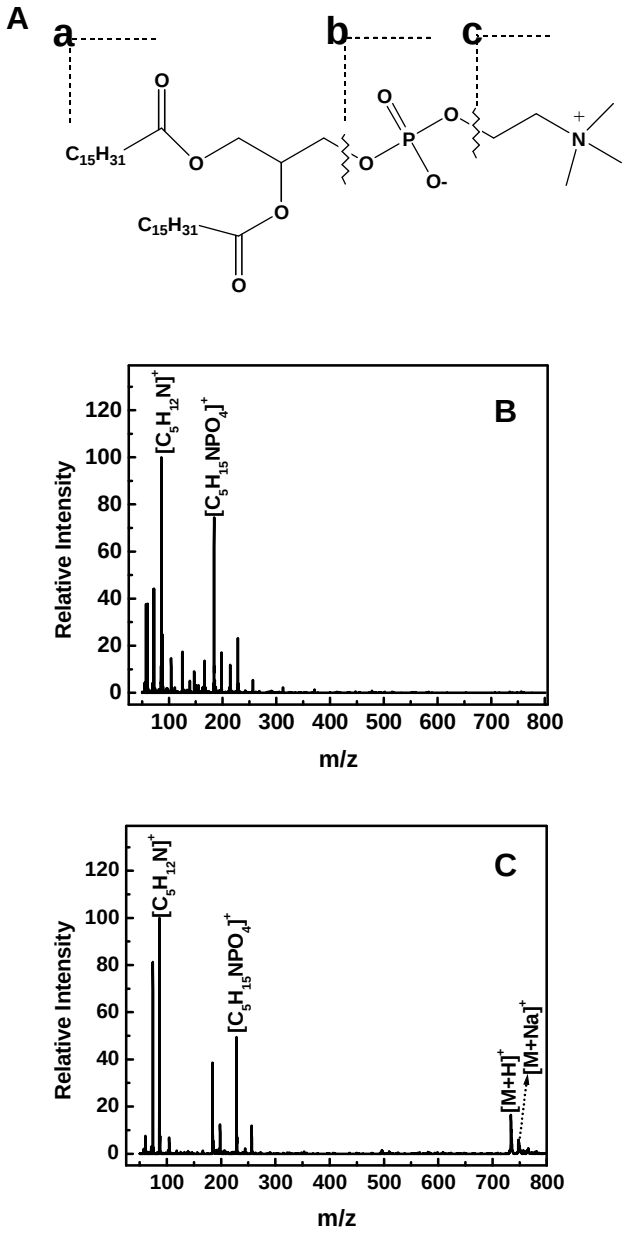

Figure 4.1 (A) Chemical structure of DPPC and the corresponding major fragments. Mass spectra of DPPC detected (B) directly on DIOS and (C) atop of Oxidized DIOS(45 min).

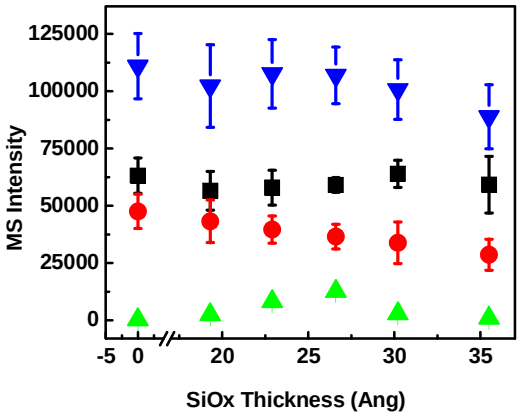

Figure 4.2 Plot of MS intensities of DPPC fragment ions m/z 184.1 (■), m/z 86.1 (●) DPPC molecular ion (▲) and TIC (Total ion current) (▼) at varied SiOx film thicknesses. All data were colleted at constant laser flux, further information see experimental section.

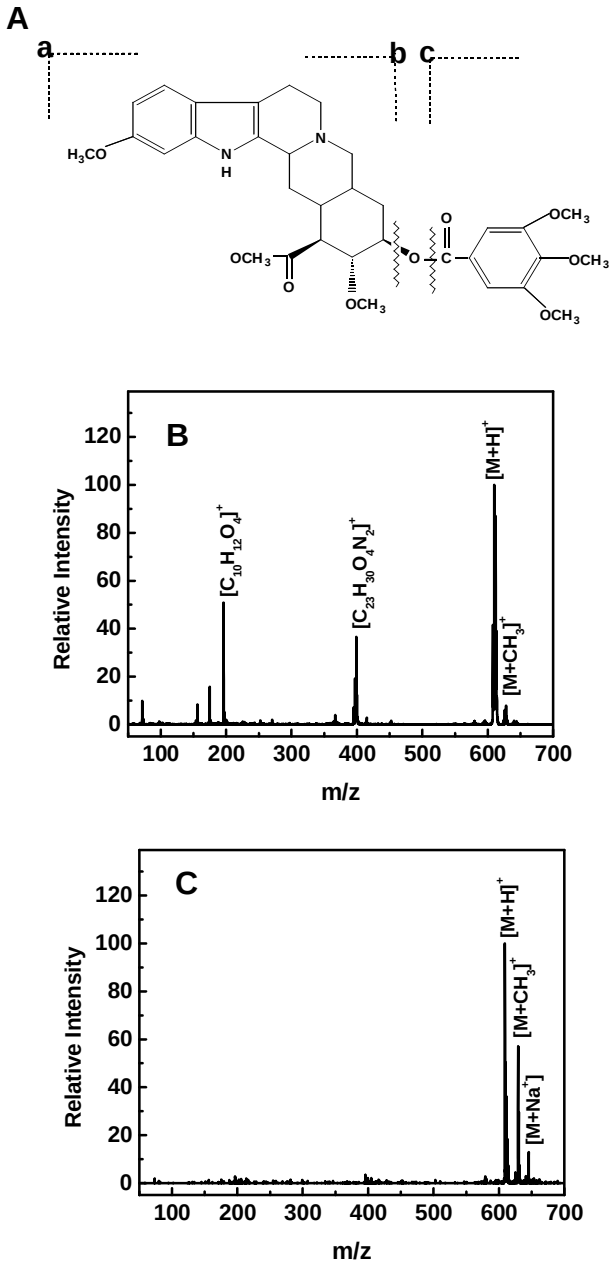

Figure 4.3 (A) Chemical structure of Reserpine and the corresponding major fragments. Mass spectra of reserpine detected (B) directly on DIOS or (C) atop of oxidized DIOS (45 min).

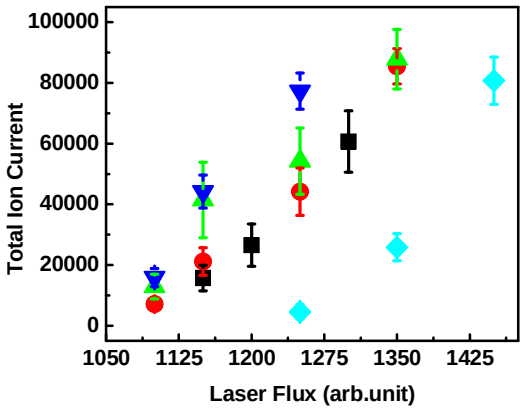

Figure 4.4 A plot of total ion currents of reserpine as a function of varied laser fluence for 0 (■), 30 (●), 45 (▲), 60 (▼), and 120 min (♦) oxidation time, respectively.

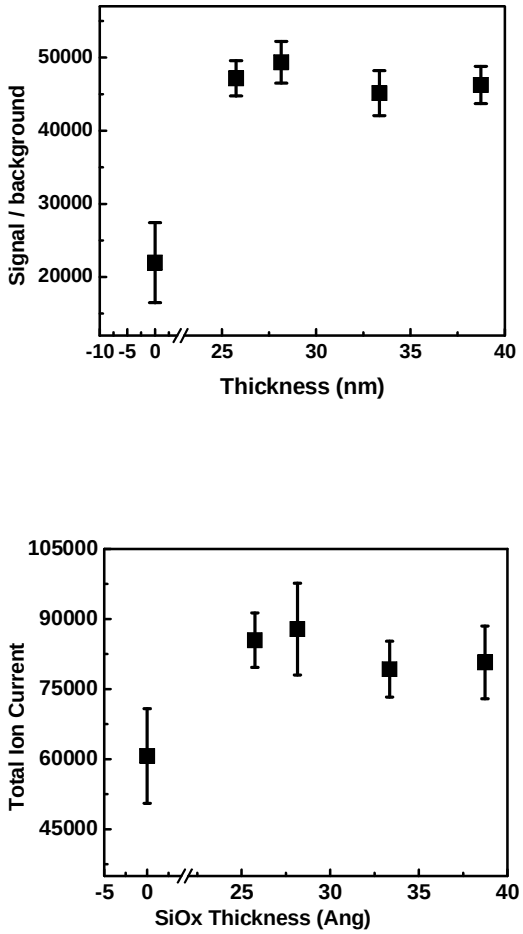

Figure 4.5 (A, B) plot of Best S/B values and total ion current of reserpine molecular ion obtained for each SiOx film thickness.

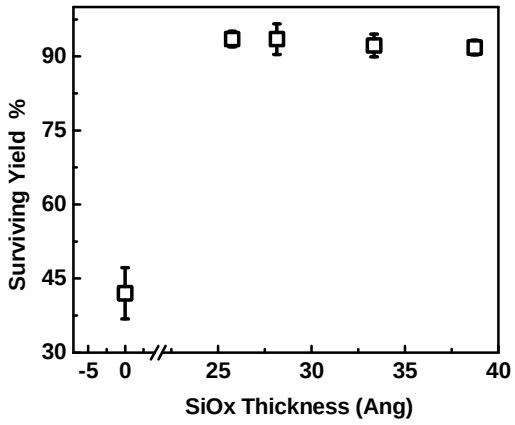

Figure 4.6 Plot of percent of surviving yield of reserpine molecular ion as a function of the each SiOx film thickness.

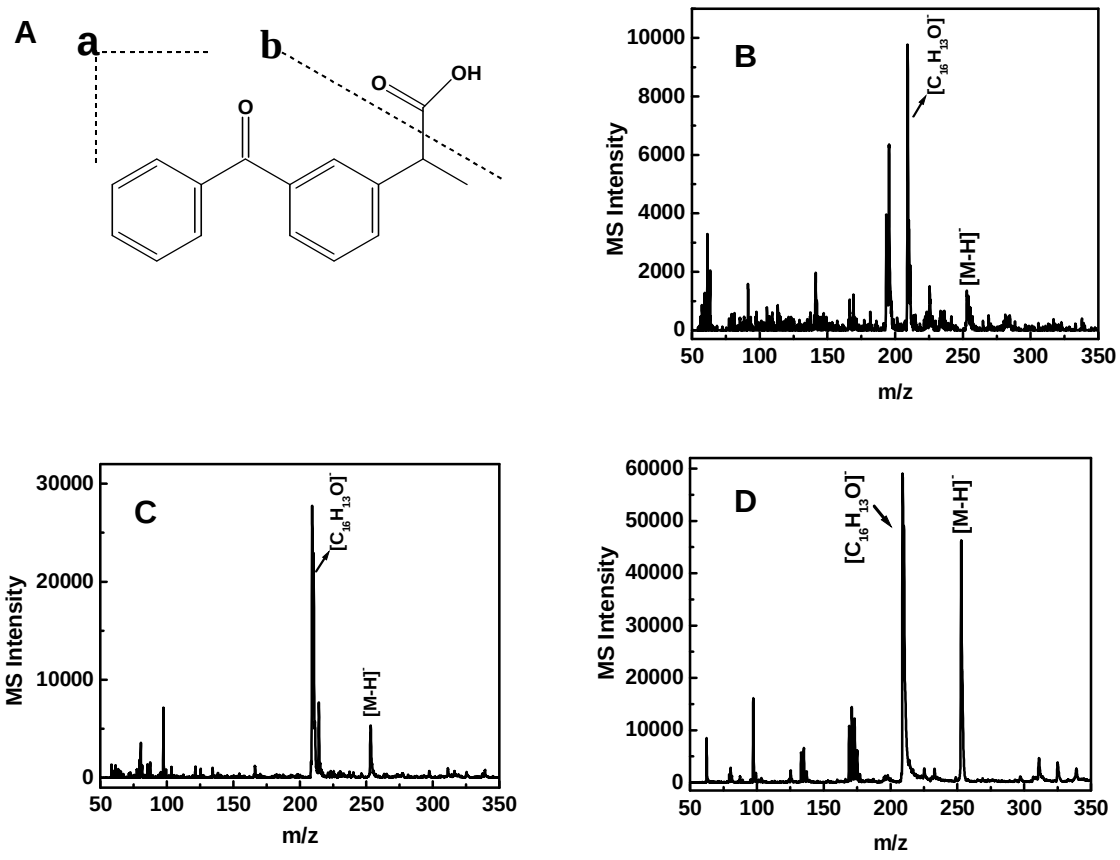

Figure 4.7 (A) Chemical structure of ketoprofen and the corresponding major fragment. Mass spectra of ketoprofen detected (B) directly on DIOS (C) on oxidized DIOS and (D) atop of APTMS derivatized DIOS.